The development of CVD-Diamond Detectors for Nuclear and HE Physics Research and its Impact to Related Fields

E. Berdermann , GSI Helmholtz Zentrum für Schwerionenforschung

Acknowledgments

Cooperators

HadronPhysics Collaborations

HGF Detector Portfolio Group

The RD42 Collaboration

Diamond Detector Users:

GSI, CERN, CEA, LAL, ...

Industrial Partners

Element Six

Diamond Materials

MICRON Semiconductors

(incorp. Diamond Detectors Ltd)

Funding

EC (FP6, FP7) HadronPhysics$_{1\text{-}3}$

NoRHDia

CARAT

Advanced Diamond Detectors

ADAMAS

Advanced Diamond Assemblies

EC (FP7) Marie Curie

MC PAD

HELMHOLTZ GEMEINSCHAFT

Outline

- Objectives
- 'Detector Grade' CVD-Diamond Materials
- Technologies and Characterization of CVDD Detectors
- Main Applications in HE and Nuclear Physics
- Selected Applications in Related Fields
- Conclusions and Outlook

Objectives

Radiation hard, ultra fast detector systems

for experiments with high-intensity 'hadron' beams

- beam diagnostics
- particle tracking and TOF
- ion spectroscopy/calorimetry

Parameters ➡ **ΔE, E, T, (x,y)**

Particles ➡ **p, e, n, HIs, X-rays**

CVD Diamond Growth Process

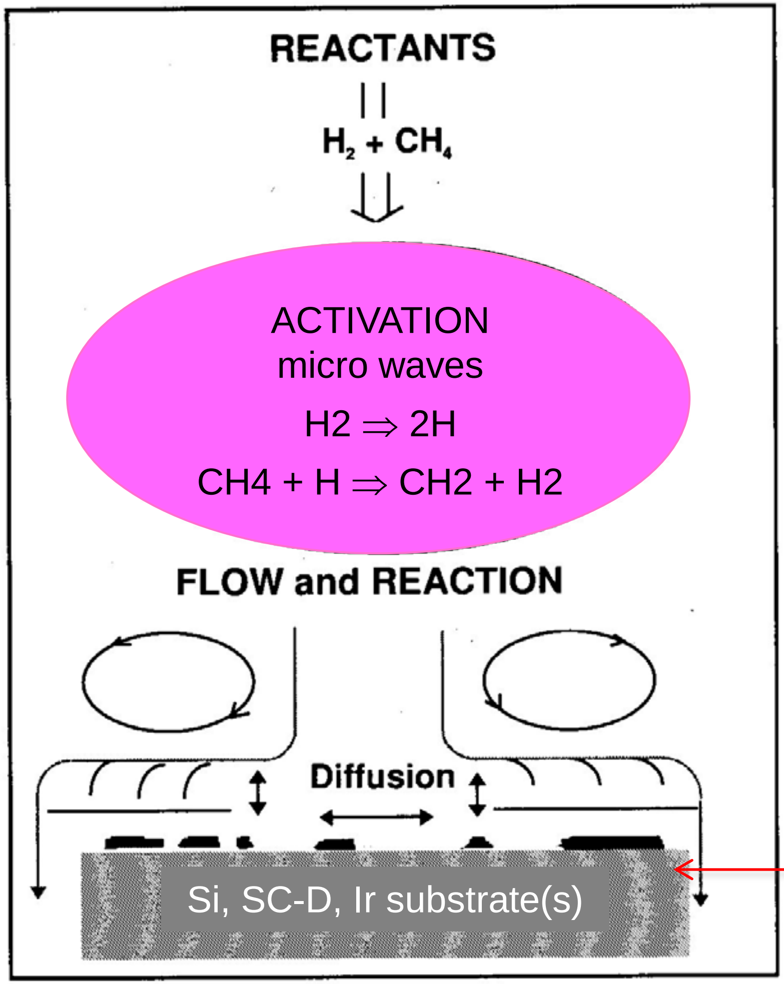

$99\%\ H_2 + 1\%\ CH_4$

micro-wave activation

Diamond + Graphite

The growth substrate defines the final crystal structure

DG CVD-Diamond Materials

- <u>Polycrystalline PCD</u>
  Areas: up to 5 inch wafer
  CCE: (typ.) ≤ 30%; (DG) ≈ 60%

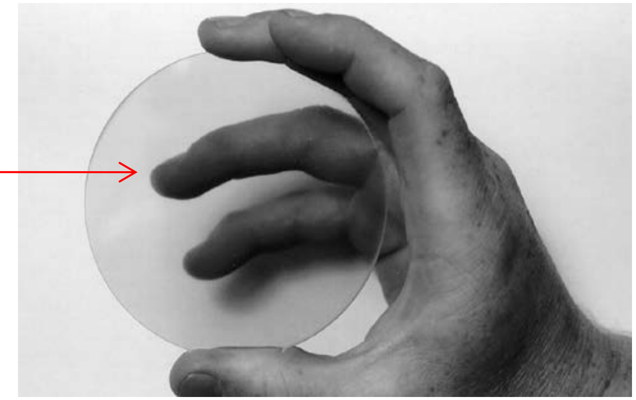

- <u>Homoepitaxial HSCD</u>
  Areas: (max.) 10 mm x 10 mm
  CCE > 98%

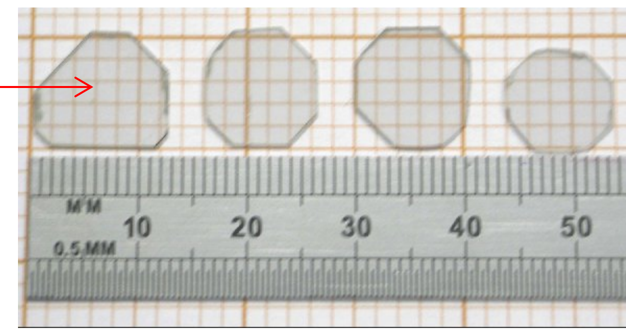

- <u>SC Dia-on-Iridium (DOI)</u>
  Areas (target): up to 4 inch wafer
  CCE (typ.) >> 70%; (best) ≥ 93%

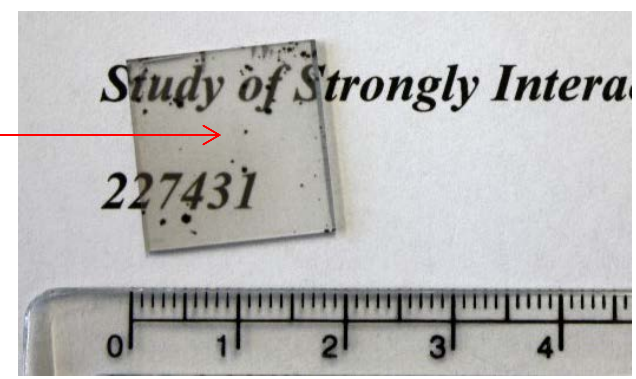

Thickness of all types: 5 - 500µm

CVDD Physical Properties

PARAMETER	CVDD	SILICON	GaAs
Z	6	14	32
ρ [g/cm^3]	3.5	2.3	5.316
$d_{Lattice}$ [Å]	3.57	5.43	5.65
σ_W $^{(300K)}$ [Wcm^{-1} K^{-1}]	20	1.3	0.55
E_{gap} $^{(300K)}$ [eV]	5.45	1.17	1.42
$E_{displacement}$ [eV]	45	24	17 -18
energy/e-h [eV]	13.1 (12.84)	3.6	4.2
X_0 [cm]	12	9.4	2.3
dE/dx [keV/µm]	0.47	0.38	0.75
ε_r	5.7	11.9	12.9
E_{break} [V/cm]	10^7	3×10^5	$4 \cdot 10^5$
μ_0 (e-)^{300K} [cm^2/Vs]	2200-4500	1500	≤ 8500
μ_0 (e+)^{300K} [cm^2/Vs]	1600-3800	600	≤ 400

CVDD Material - Properties

Crystal Structure – Birefringence Images

Dia-on-Dia

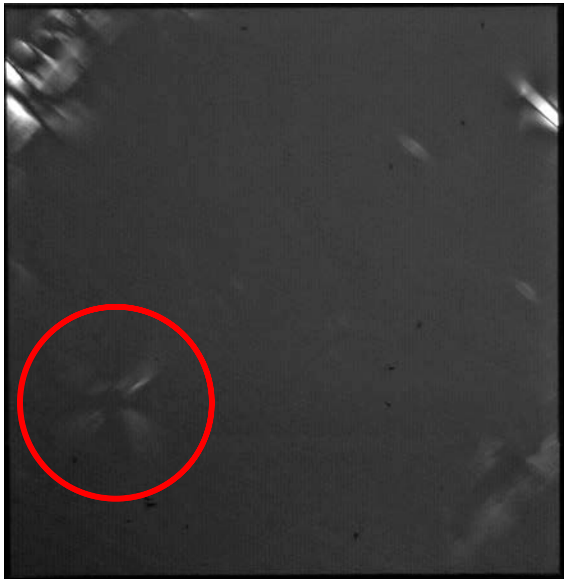

'defect-free' single crystal

Homogeneous

isolated threading dislocations + strain

Dia-on-Iridium

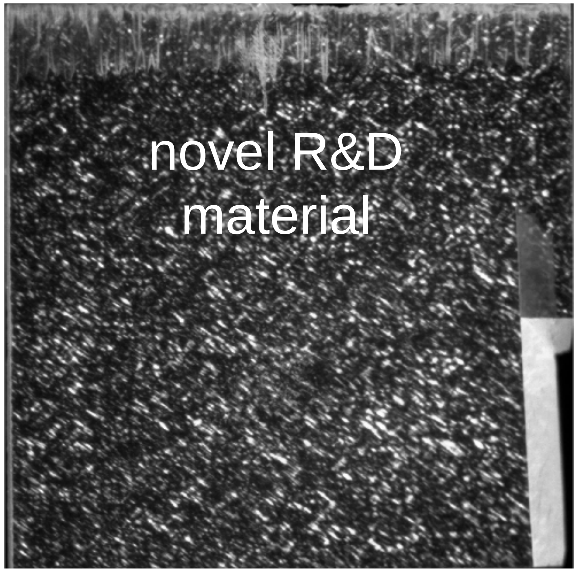

'defective' single crystal

Homogeneous

high dislocation density + strain

Dia-on-Silicon

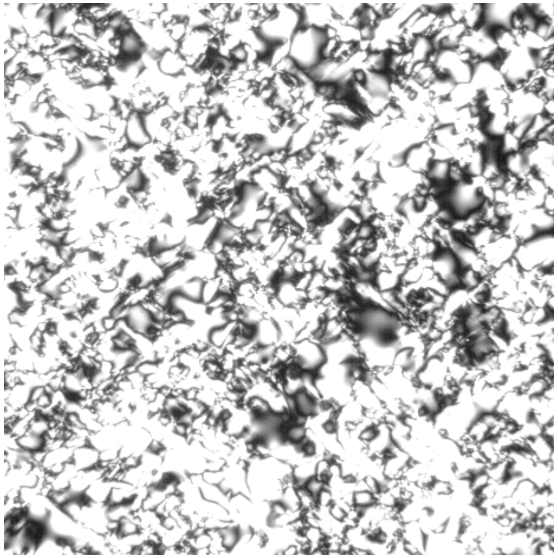

'polycrystalline'

Inhomogeneous

single crystal grains + grain boundaries

The Diamond Surface

Reconstruction: Saturation of dangling bonds by adsorbate atoms

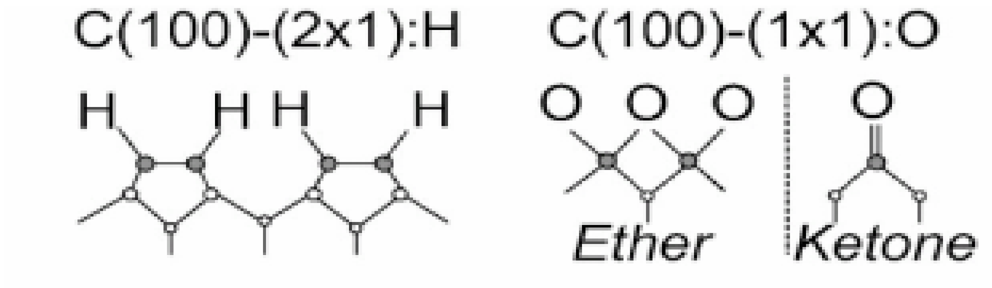

Metallization:
Diamond-contact interface

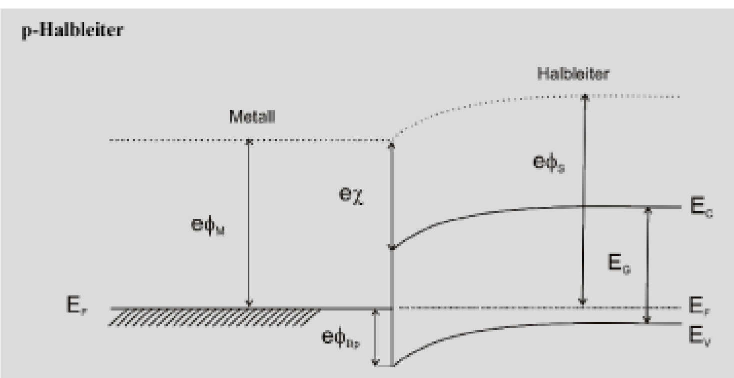

$$\Phi = E_g + \chi - \Phi_M$$

AFM image

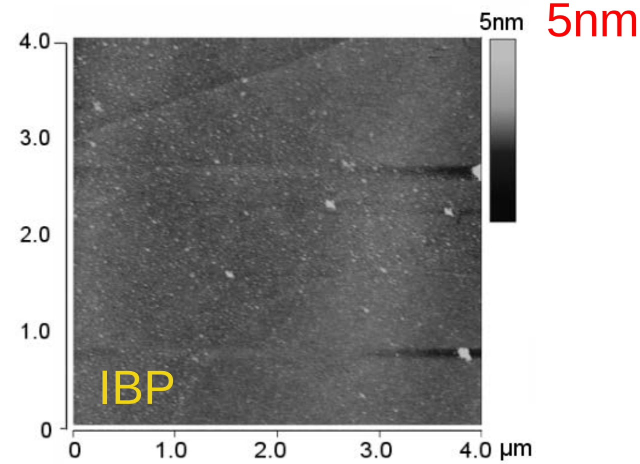

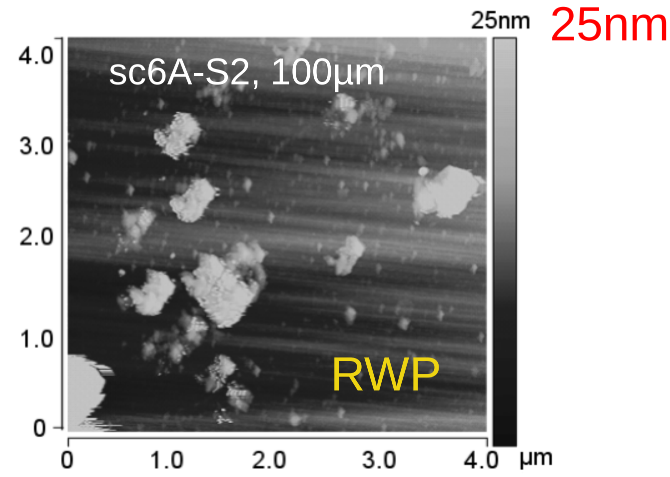

E. Berdermann et al., Diam. Relat. Mater. **19** (2010) 358-367

Technology of CVDD Detectors

Detector Electrodes – pads, strips, pixels ...

- Sputtered Ti/Pt/Au, 10min annealing at 500° C
- Sputtered CrAu; pure Al; TiW, or graphitic

Operation Principle: 'solid-state ionization chamber'

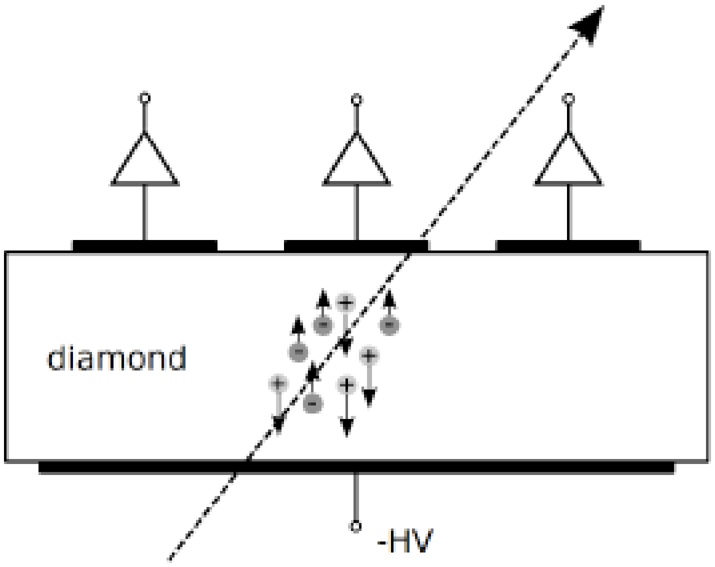

Intrinsic Diamond
- no pn-junction,
- no cooling

Drawing from Jieh-Wen Zsung, PHD Thesis, Uni Bonn, 2012

Technology of CVDD Detectors

High-frequency designs of DD for single-channel readout

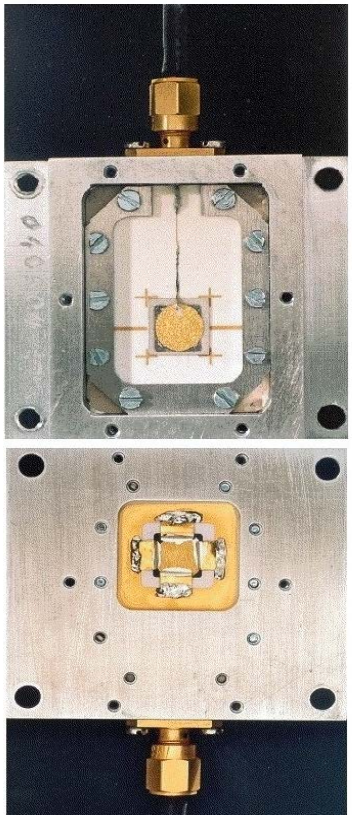

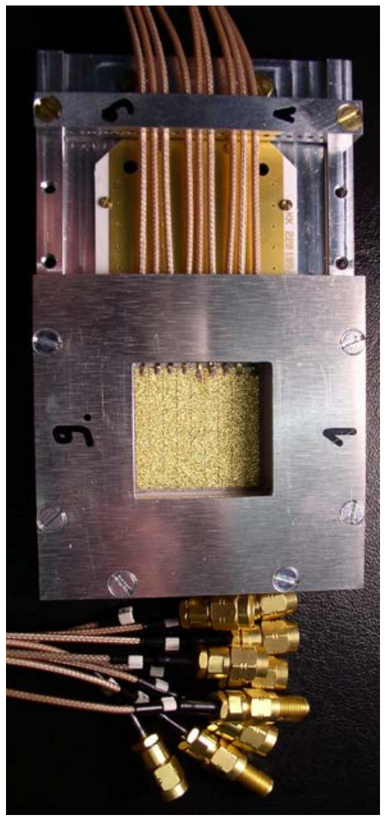

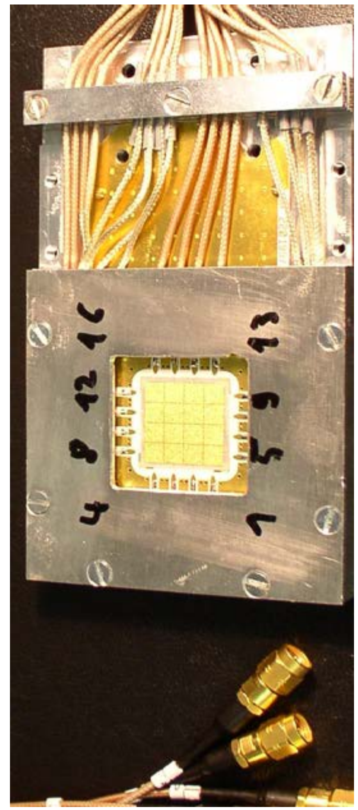

Beam-halo moni, 20mm ⃠:
a diamond-ring counter

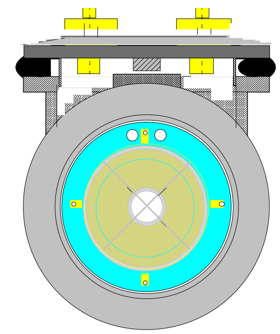

Beam-halo and START

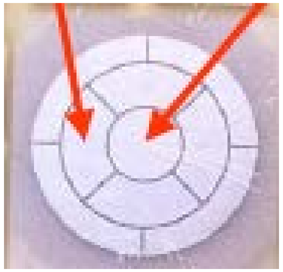

30 mm x 30 mm

- ❑ Every detector channel is a 50 Ω-micro stripline

Technology of CVDD Detectors

Multipurpose quadrant sensor for removable small-area detectors

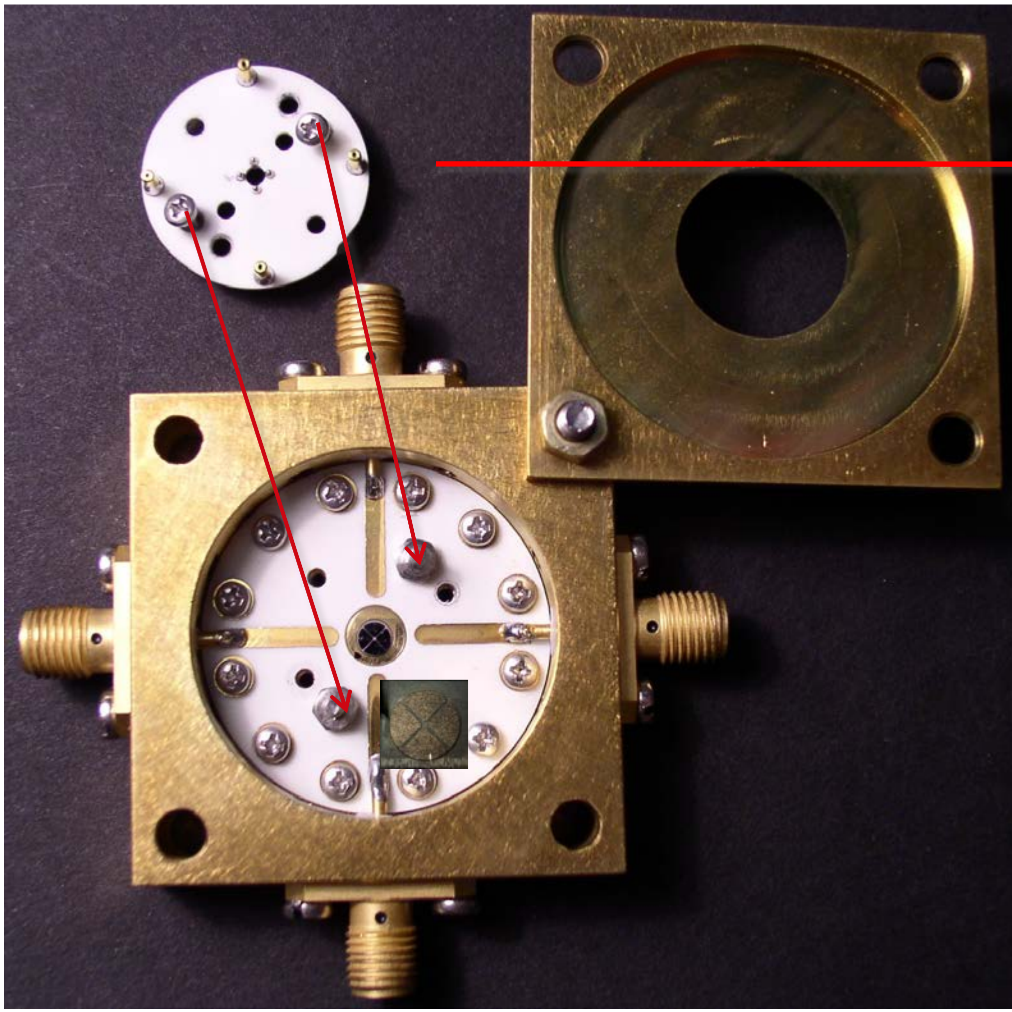

rear side

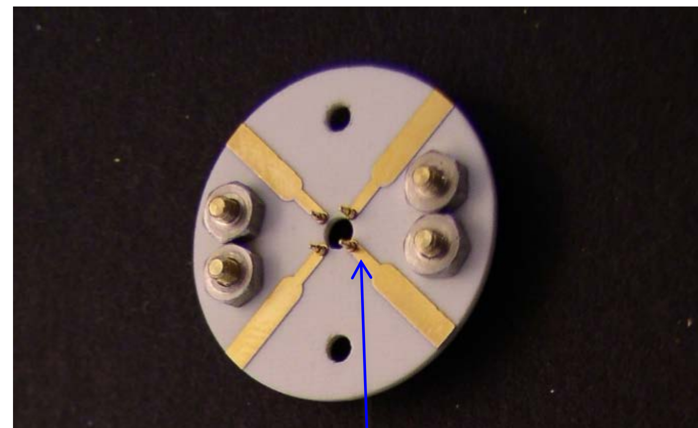

4 x mini spring-contacts

Technology of CVDD Detectors

Diamond Hybrid SC and PC Pixel Detectors
Multichannel – ASIC readout

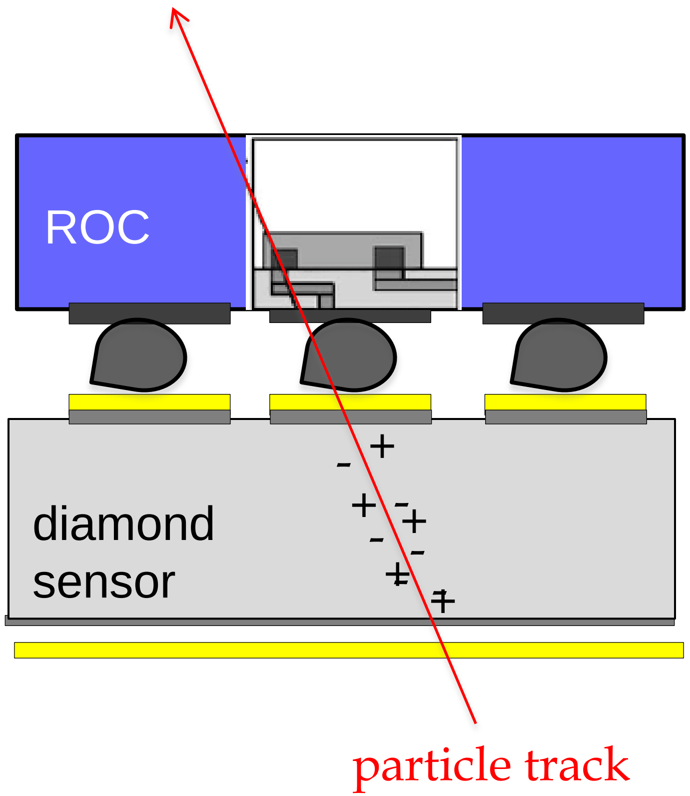

- Metallization: Ti-W (-Au),1µm
  - Bump bonding and flip-chip technology;
- ≈ 15 µm bumps (In or Sn/Ag)
- No guard rings

Characterization CVDD Detectors

IV Characteristics

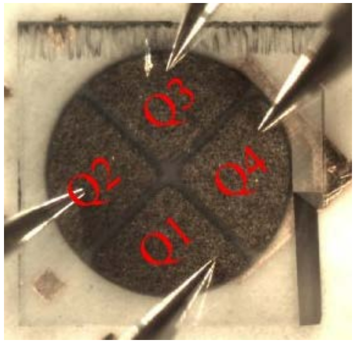

Single Crystal (HSC)

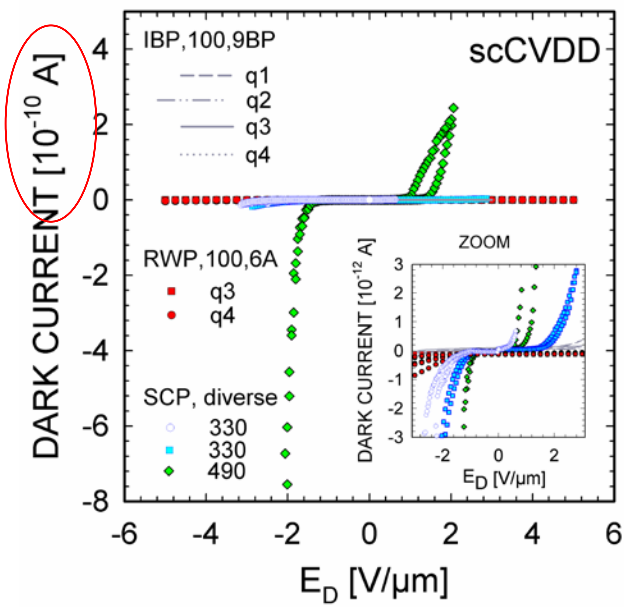

Dia-on-Ir (DOI)

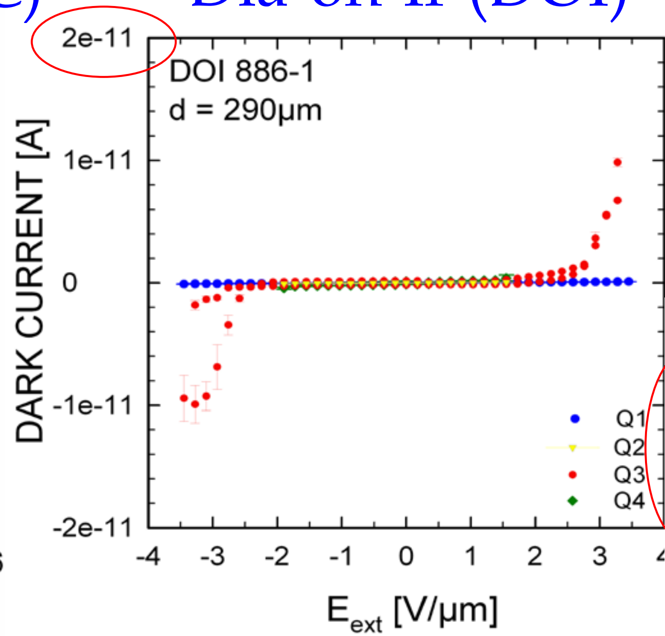

Polycrystalline (PC)

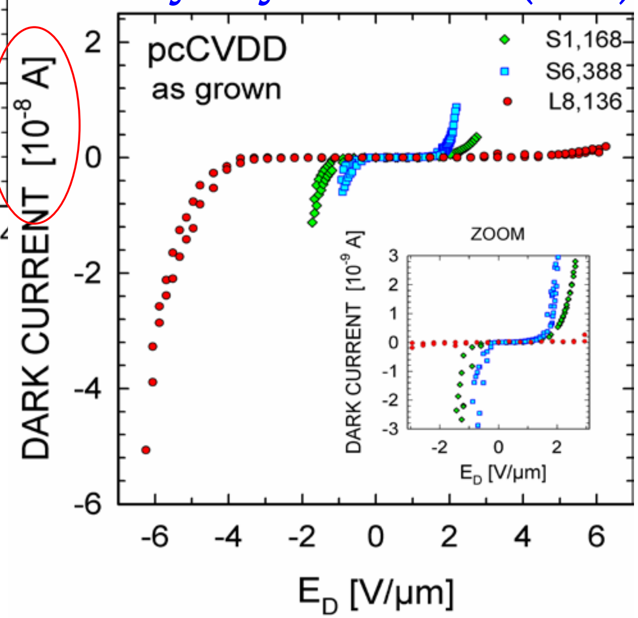

Wide band gap materials

- Low I_D up to T > 100° C

Characterization CVDD Detectors

TCT with Short-Range Particles

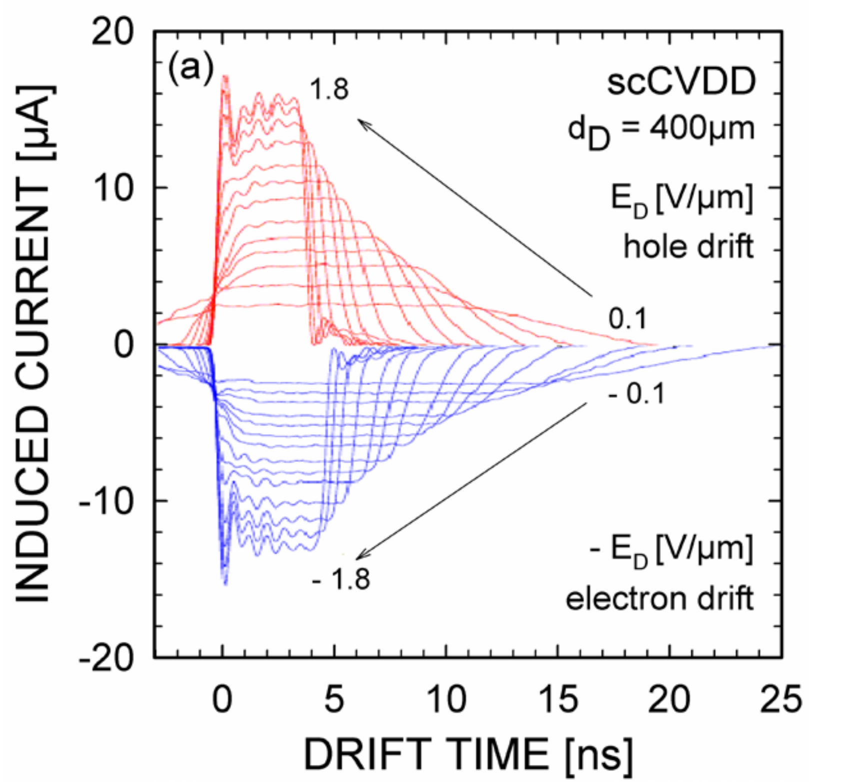

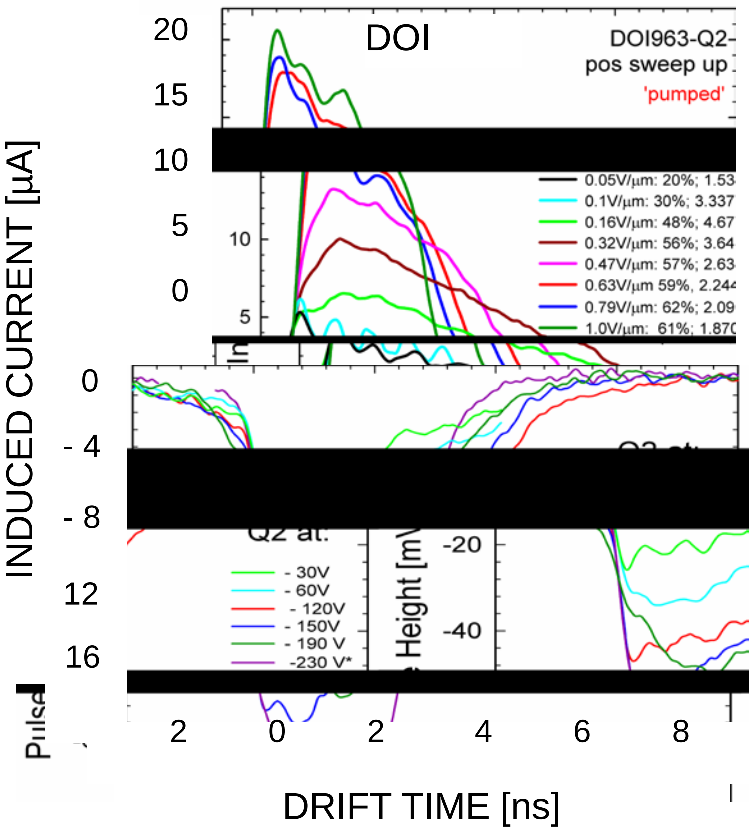

PRELIMINARY

<u>Trapezoidal signals indicate:</u>
Homogeneous internal field profile;
Complete Q drift to the opp. electrode

<u>Flat-top slope indicates:</u>
net eff. space charge;
charge trapping

Characterization CVDD Detectors

CS measurements with ^{90}Sr electrons of $E_ß$ > 1MeV

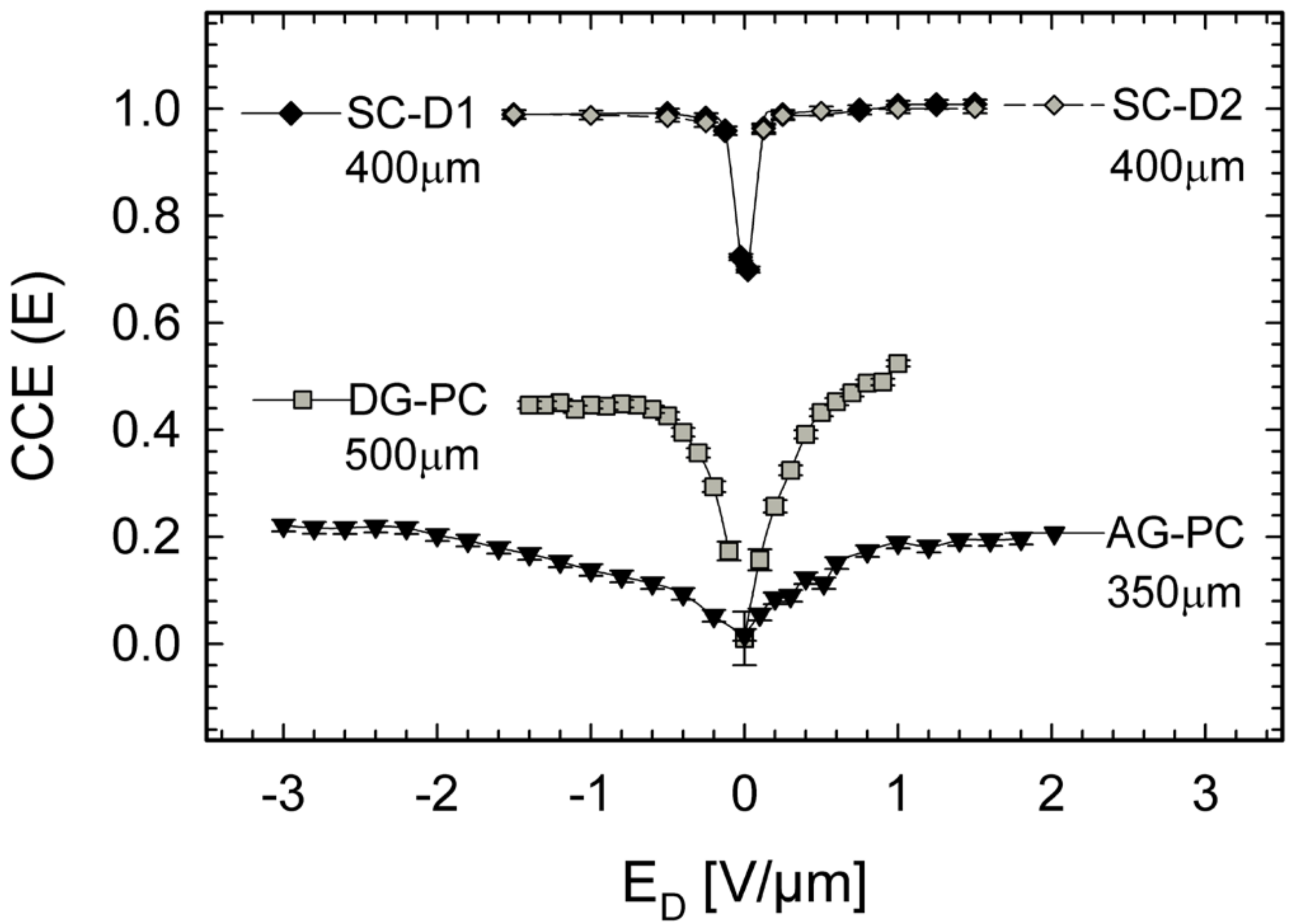

Transport Parameters and Lifetime

TCT (α)

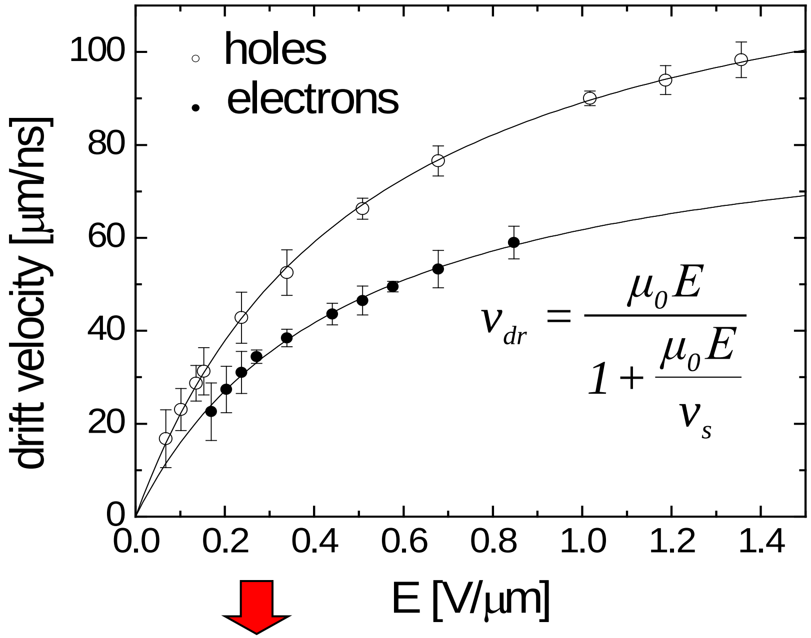

Transport parameters

v^e_s = (0.85 ± 0.08) x 10^7 cm/s;

μ_0 = (2071 ± 212) cm^2/Vs

v^h_s = (1.34 ± 0.05) x 10^7 cm/s;

μ^h_0 = (2630 ± 123) cm^2/Vs

TCT (α) + CCE (^{90}Sr)

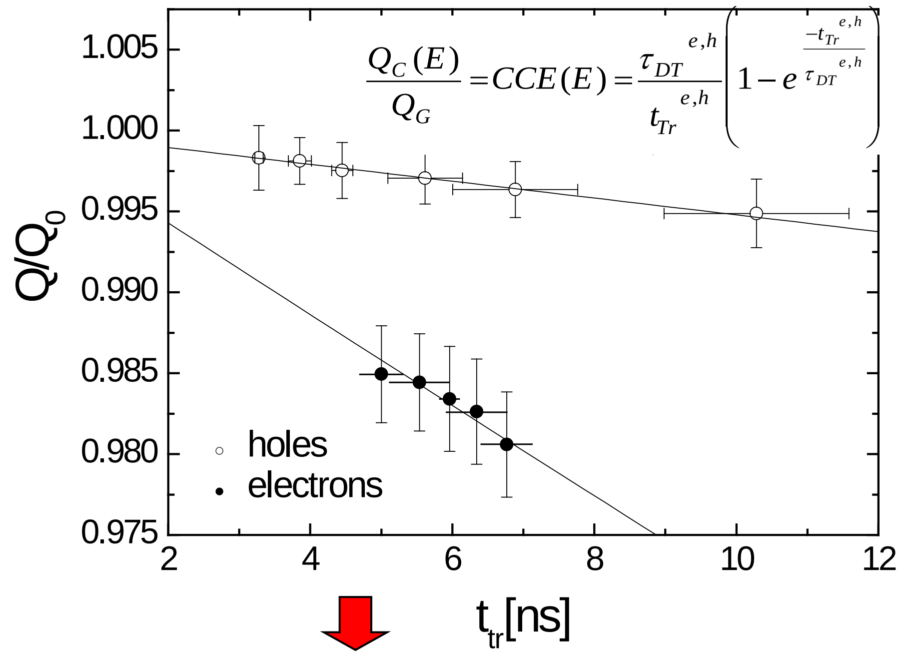

Carrier lifetime

τ^e = 174 ± 15 ns

τ^h = 968 ± 230 ns

M. Pomorski et al., phys. stat. sol. (a) 202, no. 11, pp. 2199

Characterization CVDD Detectors

Energy and Energy Loss resolution

Compare HSC, PC

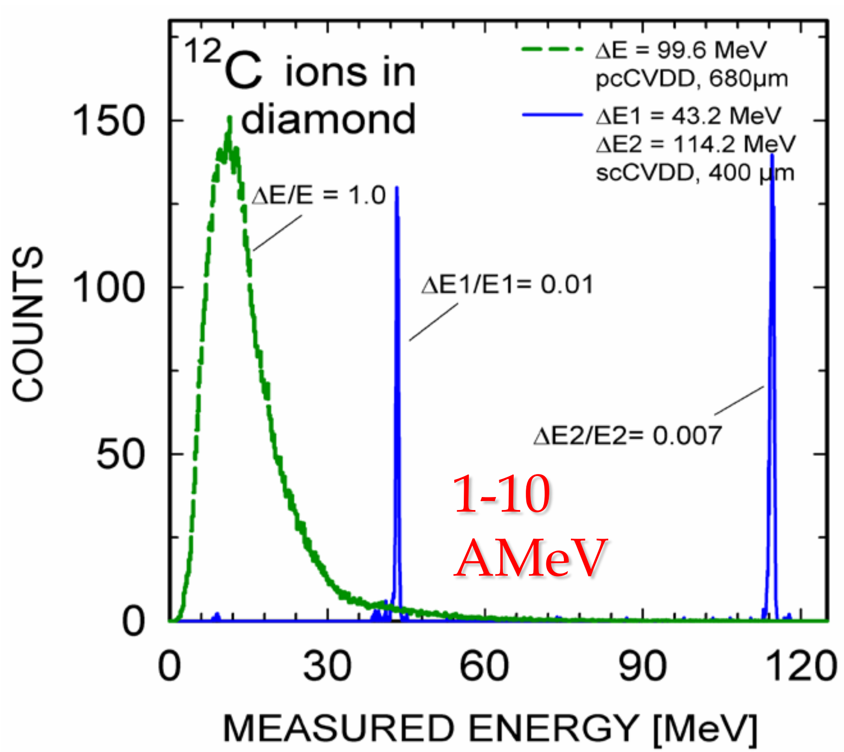

Compare SC, Silicon

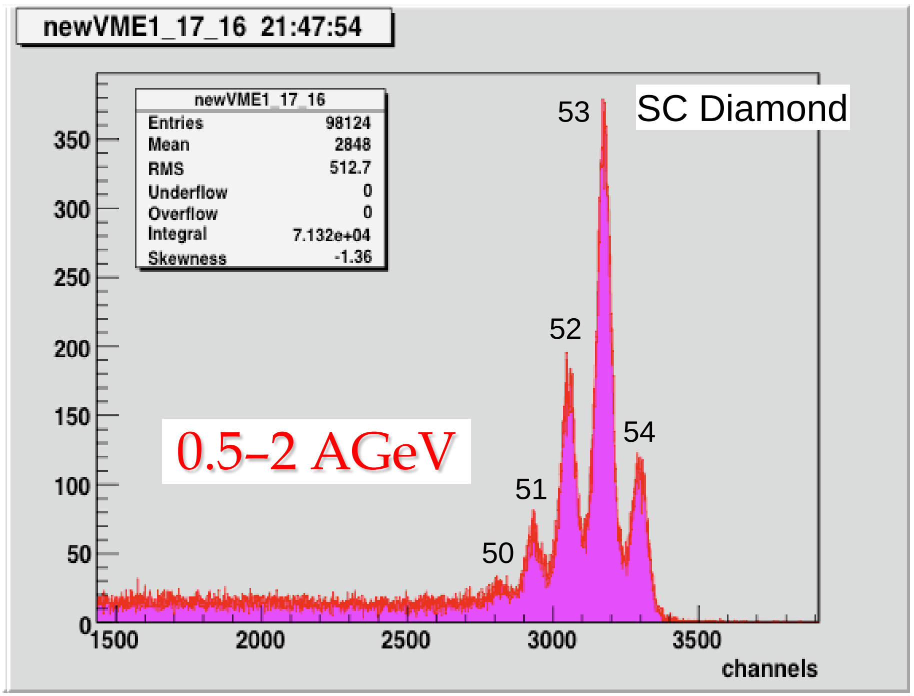

pcCVDD: no E resolution

scCVDD: superior δE/E to Si

E. Berdermann et al., Diam. Relat. Mater. **17** (2008) 1159

Intrinsic TOF resolution

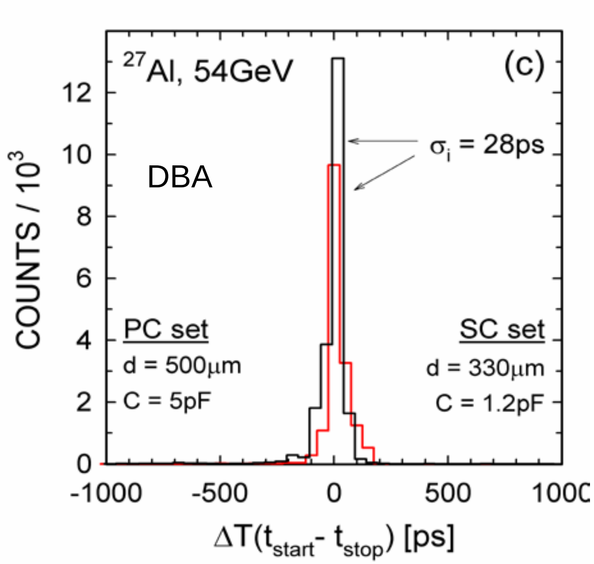

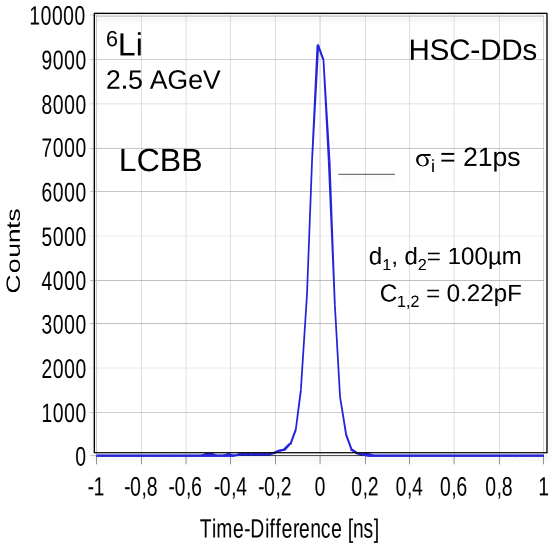

$\sigma_i^{ions} \leq 25$ ps

limited by bandwidth and noise of available BB FEE

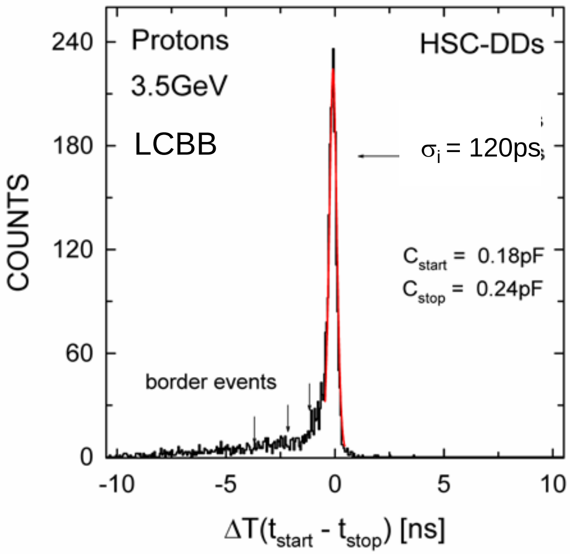

$\sigma_i^{proton} \approx 100$ ps

limited by the bad S/N ratio for MIPs

E. Berdermann, M. Ciobanu et al., Proc. IEEE NSS (2009) Orlando

Characterization CVDD Detectors

Radiation hardness studies

M. Pomorski, PhD Thesis (2008)

Charge Collection

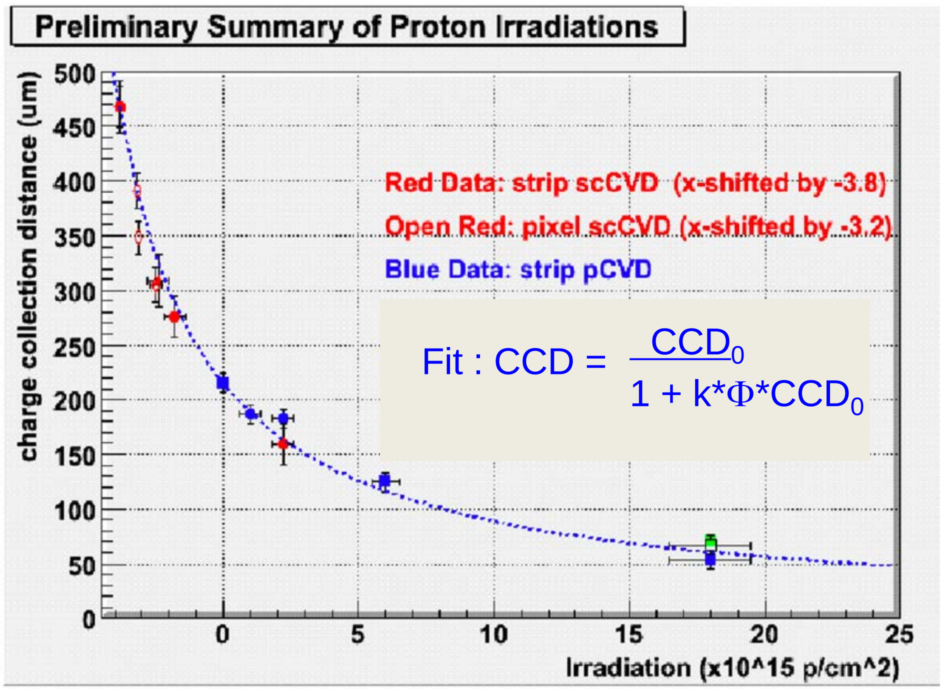

The RD42 Collaboration (2008)

Thickness Dependence

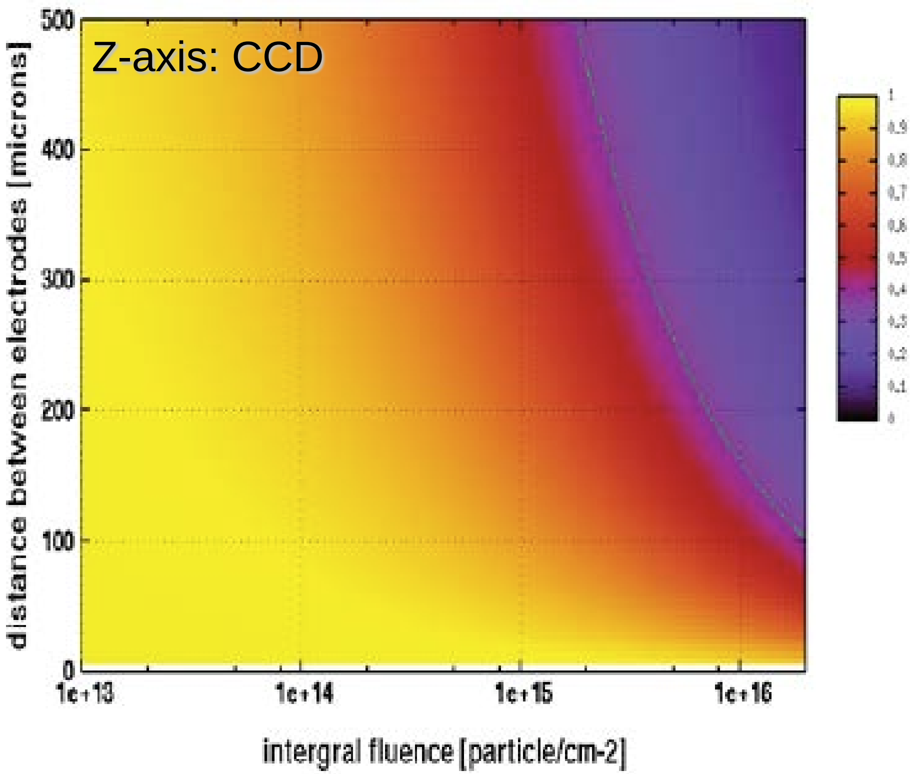

- thinner = 'harder'

Characterization CVDD Detectors

Damaged HSC Samples

M. Pomorski, PhD Thesis (2008)

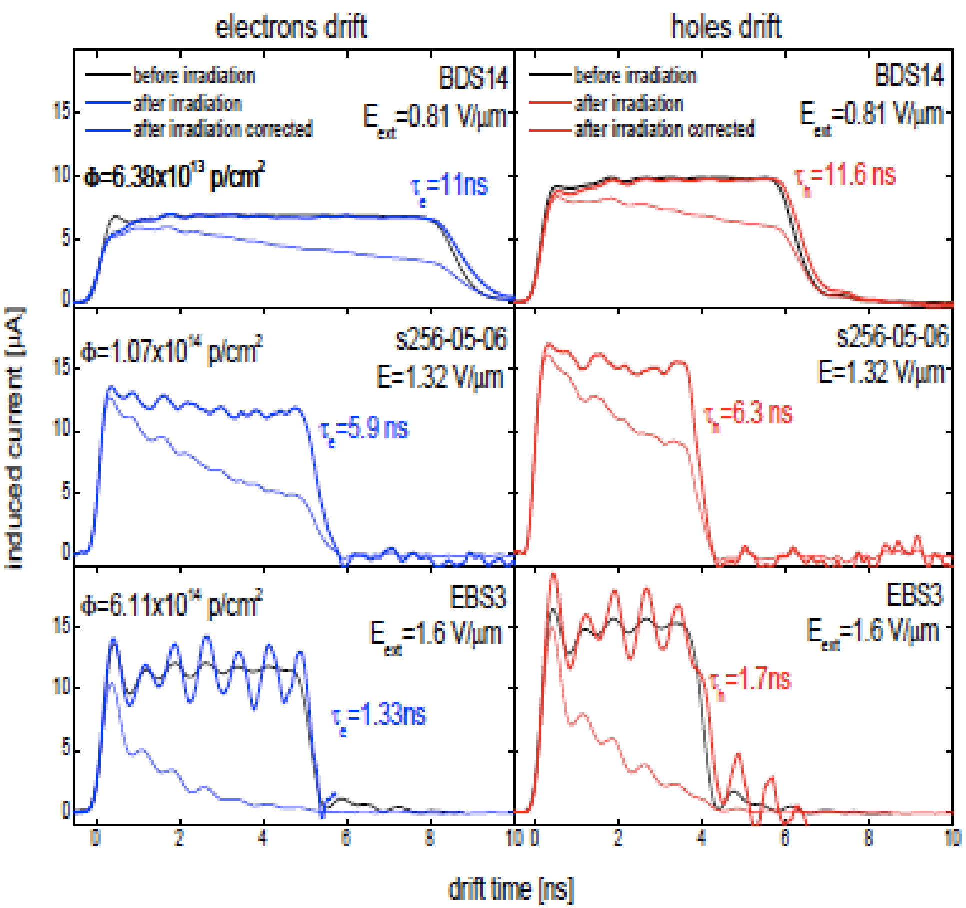

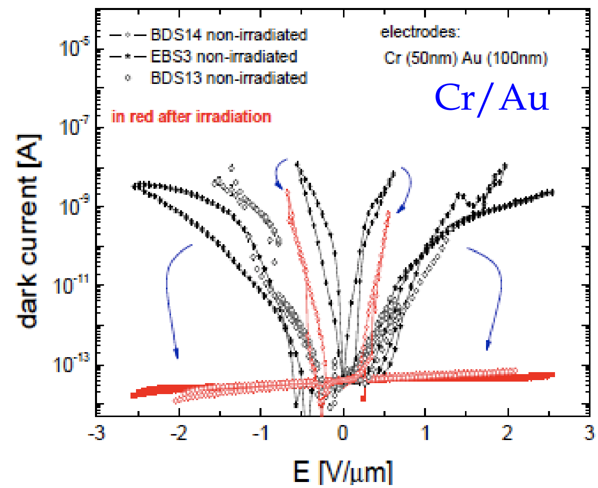

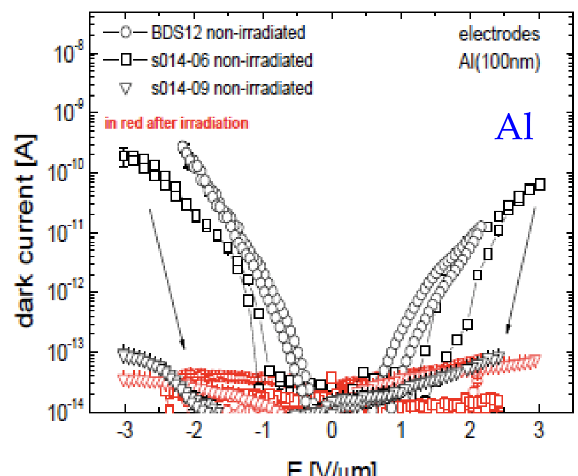

- TCT indicate V0 production
- Timing signal 'harder' than CCD

- Compensation of shallow traps by deep V^0

Applications in Nuclear and HE Physics:
Diamond Detectors for GSI, FAIR, and LHC

In-beam START-VETO detectors for HADES and CBM

HI, T0 sensor

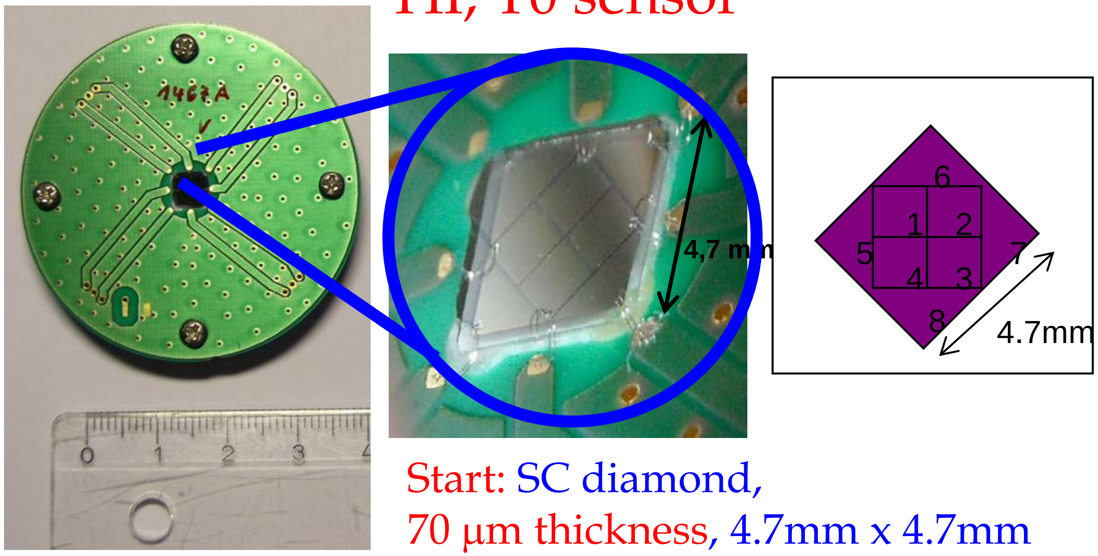

Start: SC diamond,
70 μm thickness, 4.7mm x 4.7mm

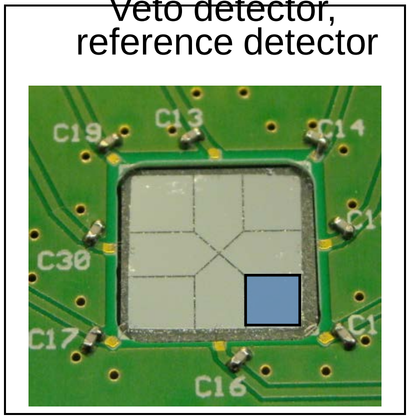

Veto: PC diamond,
100 μm thickness, 20 mm x 20 mm

J.Pietraszko, 21st CBM Collaboration Meeting

HI and MIP Detectors for GSI / FAIR

CBM ➡ The challenge: 10^9 part/s → 10^7 interactions/s; beam spot 1mm ⃠

- SCD $d_D \leq 50\ \mu m$ thickness
- Areas of several cm^2
- Single-ion beam tracking
- Time resolution < 50 ps

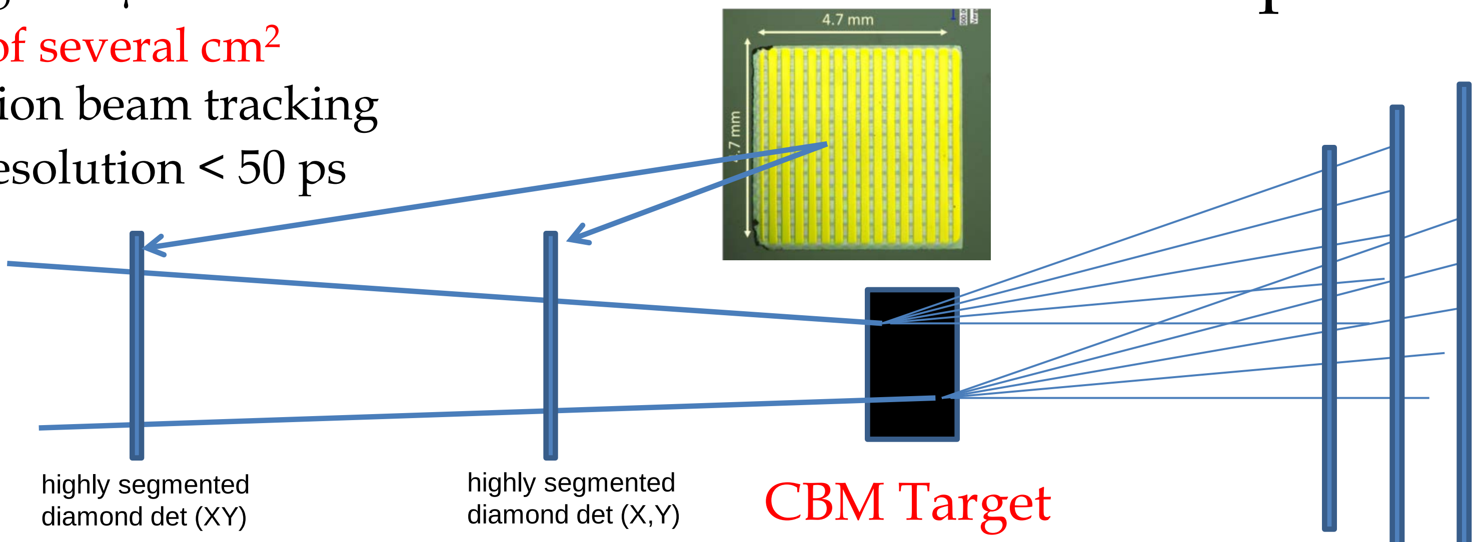

❑ Double-sided multi-strip diamond sensors (16 strips each side)

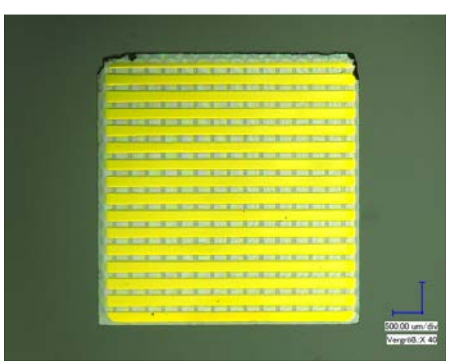
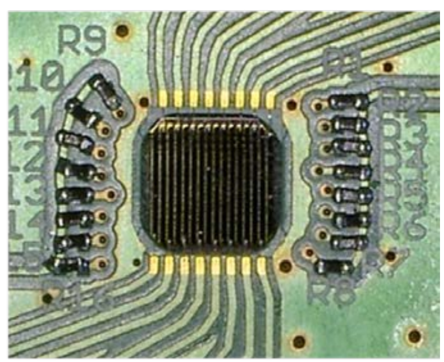
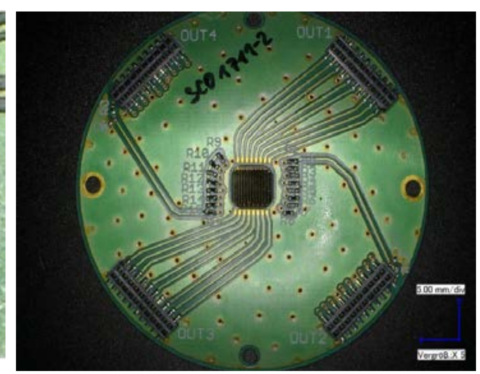

290 µm pitch
$d_D \approx 60\ \mu m$

J. Pietraszko, 21st CBM Collaboration Meeting

HI and MIP Detectors for GSI / FAIR

Tracking and TOF Detectors for Experiments with Radioactive Beams at the SFRS/FAIR

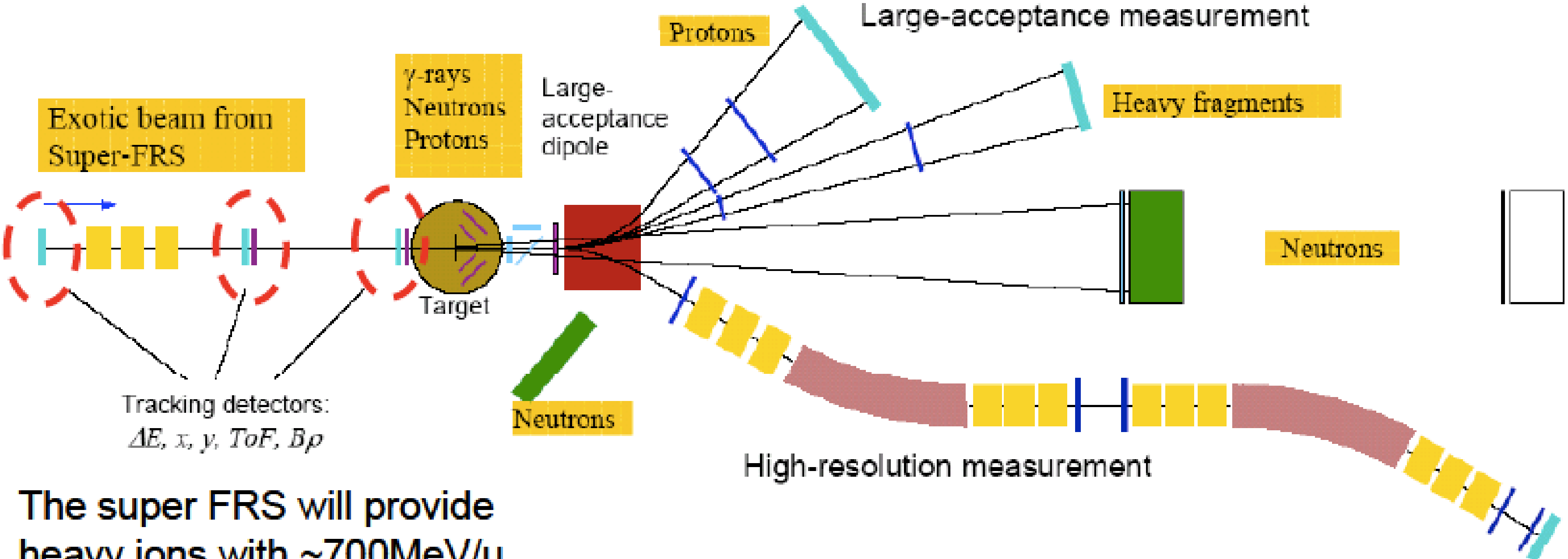

The super FRS will provide heavy ions with ~700MeV/u

Measurement of all kinematic variables in a HI reaction

Different tasks: High resolution tracking in the super FRS, radiation hard (SFRS) 10^6 cm^{-1} s^{-1}

2 x TOF (SFRS – target) (reaction products)

R. Gernhäuser (TUM)

Tracking and TOF Detectors for Experiments with Radioactive Beams at the SFRS/FAIR

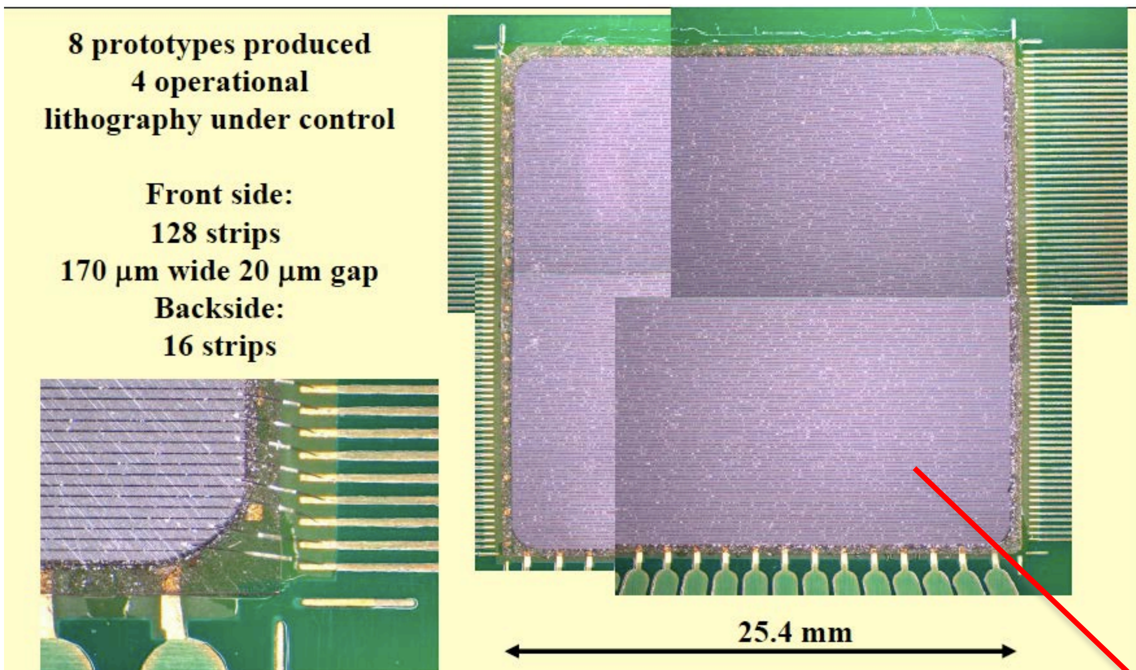

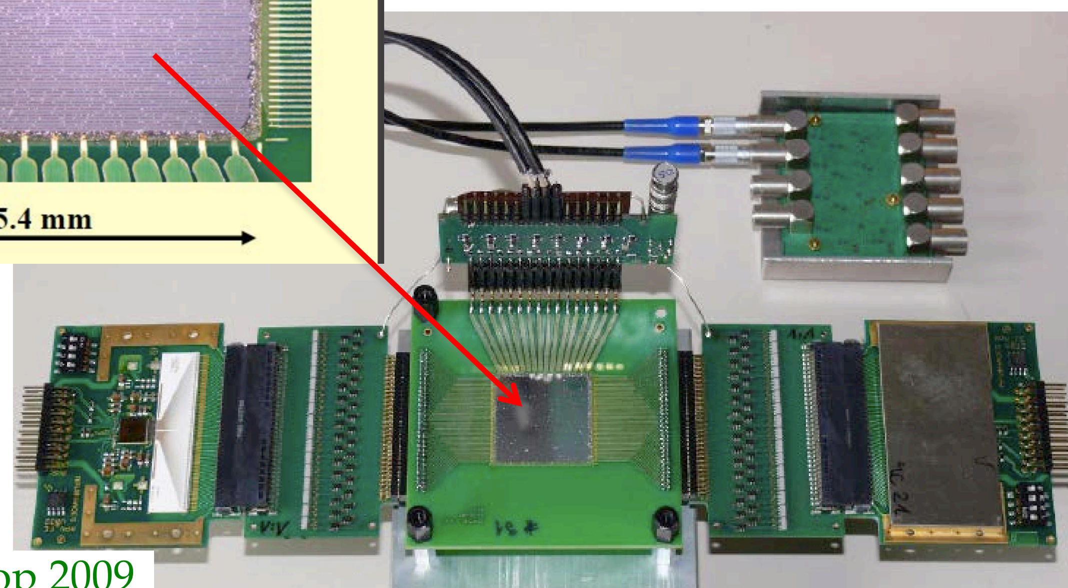

Concept:

Front-side for tracking;
Backside for TOF

R. Gernhäuser (TUM), CARAT workshop 2009

Pixel Sensors for LHC and HL-LHC

ATLAS Insertable B Layer (IBL)

Provide ATLAS with a 4-layer pixel tracker

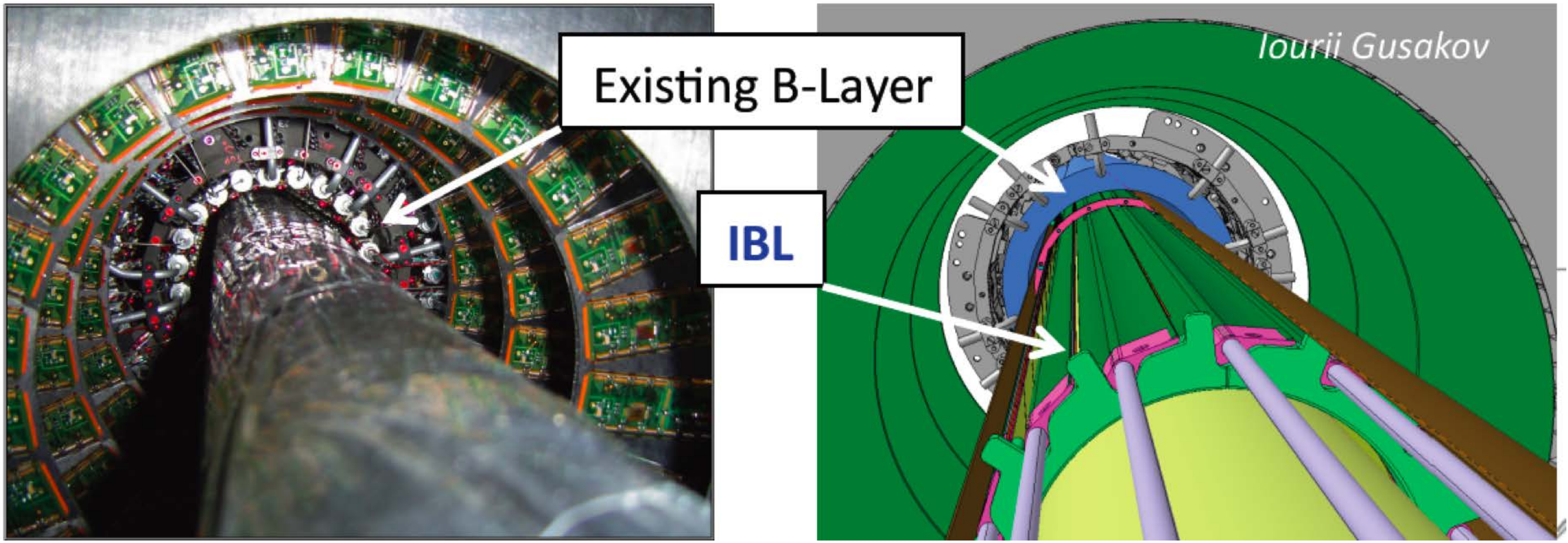

Pixel upgrade for increased L = 3×10^{34} cm^{-2} s^{-1}

Hügging, ... Wermes et al., Uni Bonn ⟶ 3 promising sensor technologies:
planar Si, 3D silicon, and polycrystalline diamond

ATLAS Diamond PC and SC Pixel Sensors

Readout Chip FE-I4:

80 x 336 pixels
50 µm x 250 µm
336 rows à 50 µm pitch
each channel C_D = (21.47 ± 0.1) fF

Sn/Ag bump bonding and flip-chip technology (e.g. at IZM)

Spatial Resolution:

- SC sensors: σ_{row}= (8.9 µm ± 0.1) µm
- PC sensors: digital res.

Sensor + FE-I4 mounted

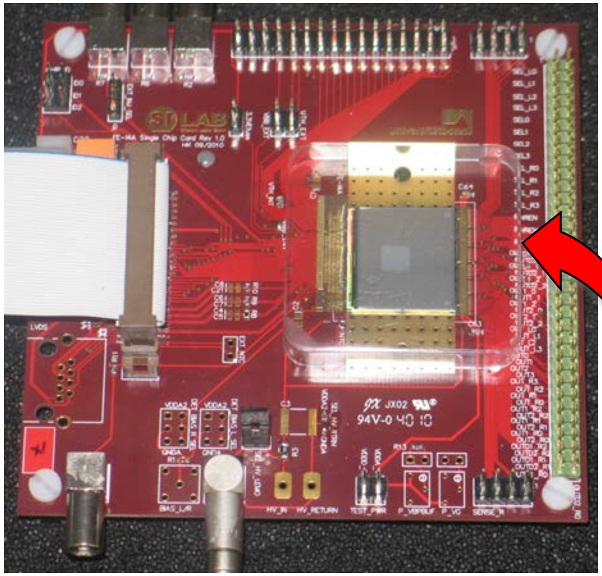

4.8 mm

4.8 mm

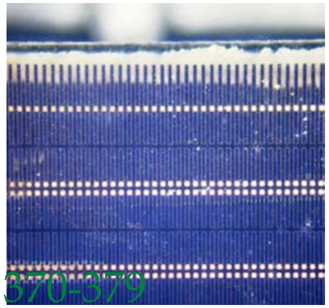

$d_D \approx 500$ µm

N. Wermes, 'Pixel detectors for charged particles', NIM A **604** (2009) 370-379
Jieh-Wen Zsung, PHD Thesis, Uni Bonn, 2012

The CMS Pixel Luminosity Telescope (PLT)

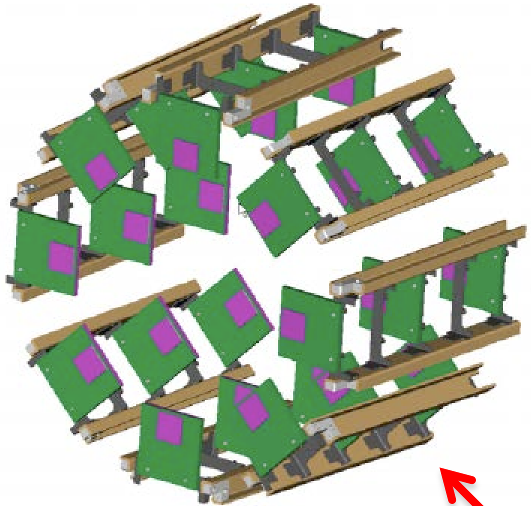

single telescope:

three planes of HSC DDs

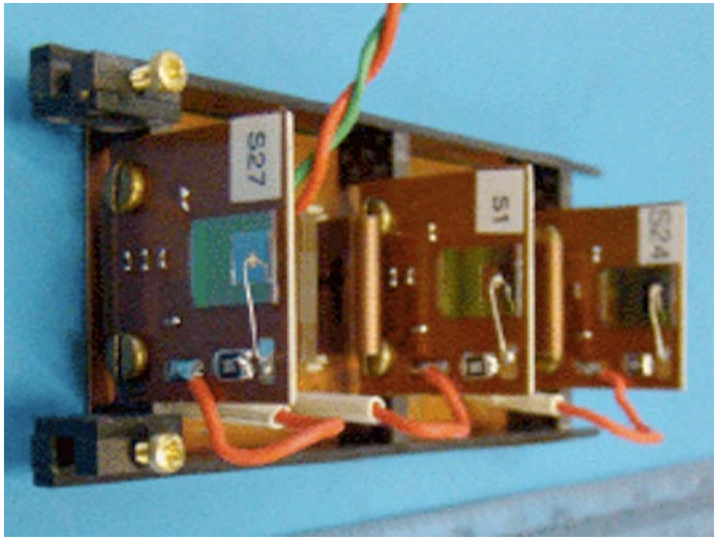

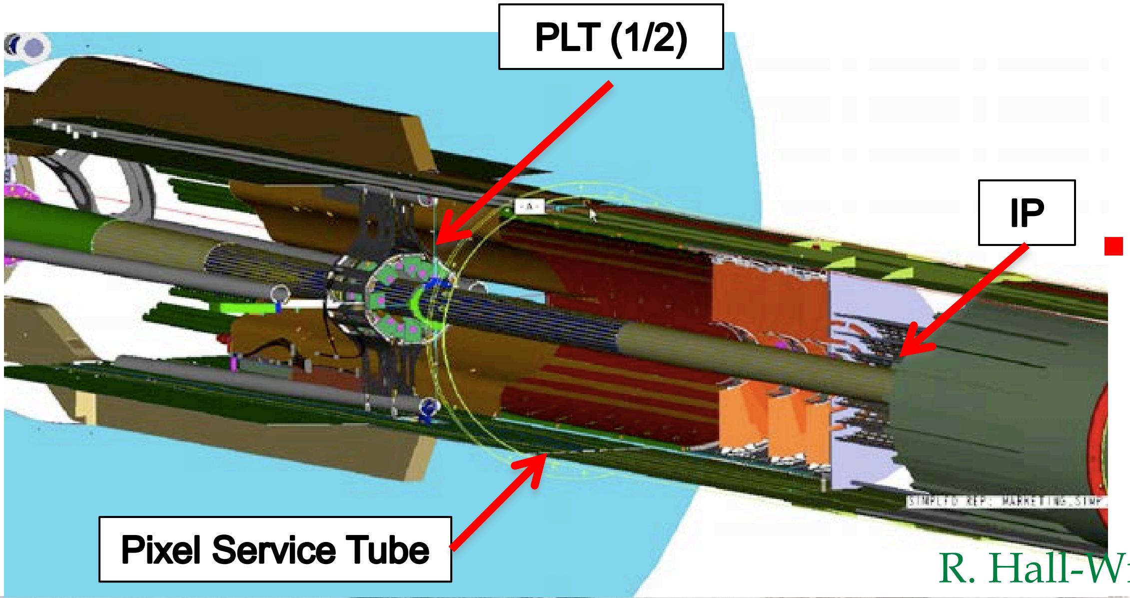

- End of Be section of beam pipe (≈ 1.7 m from IP)
- Just outside of beam pipe (≈ 5 cm from beam line)

R. Hall-Wilton et al., NIM A **636** (2011) S1 30-S1 36

CMS SC pixel detectors for the PLT

Unique dual readout capability: → PSI 46V2 chip

80 x 52 pixels,
100 μm x 150 μm
area 8mm x 7.8mm

Luminosity mode

- Fast output (40 MHz bunch-by-bunch),
- individual pixel threshold, masking …

Tracking mode

- Full pixel readout (≈ 1KHz),
- pixel address and pulse height of each hit

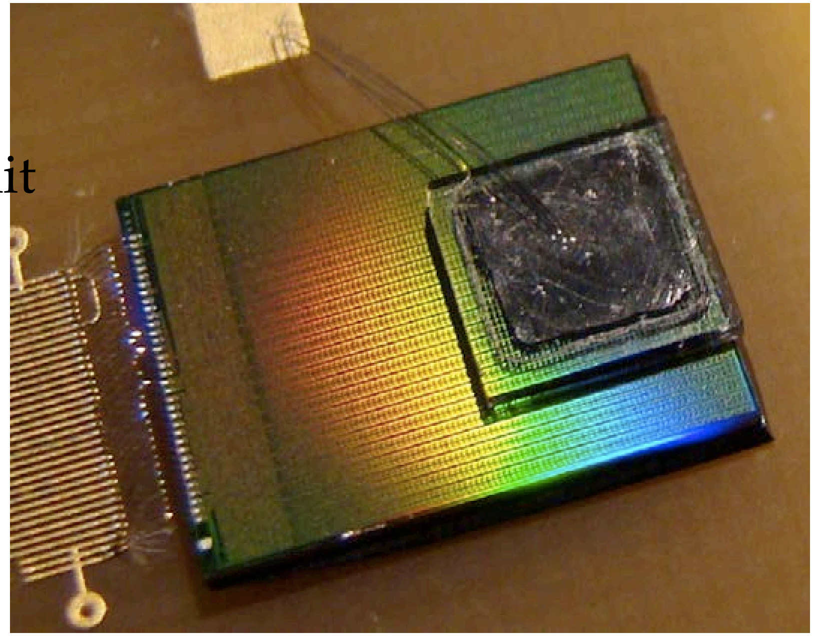

Spatial Resolution:

- σ_{row}=29 (43) μm for 2(1)-hit cl.
- σ_{col}=23 (29) μm for 2(1)-hit cl.

R. Hall-Wilton et al., NIM A **636** (2011) S1 30-S1 36

New Diamond Detector Technology

Silicon-on-Diamond (SOD) devices

Lagomarsino, Parrini, Sciortino et al., PoS(RD09)029

SOD - Principles

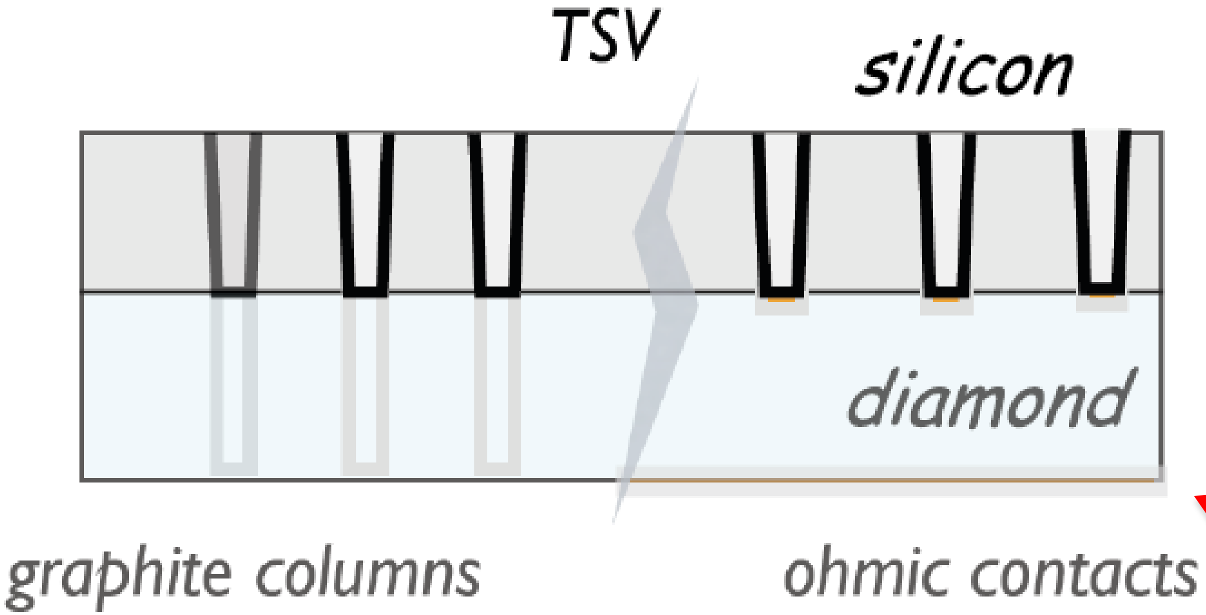

by laser bonding

1) SOD detectors for HEP
with matrices of TSV contacted with diamond by means of deep graphitic spots.

2) SOD devices with graphitic columns for biological studies as interface between a neuronal culture and a FEE for stimulation and readout.

Lagomarsino, Parrini, Sciortino et al., PoS(RD09)029

First SOD Prototype(s)

SOD pixel detector for HEP → Low-resistance Si, High quality CVDD

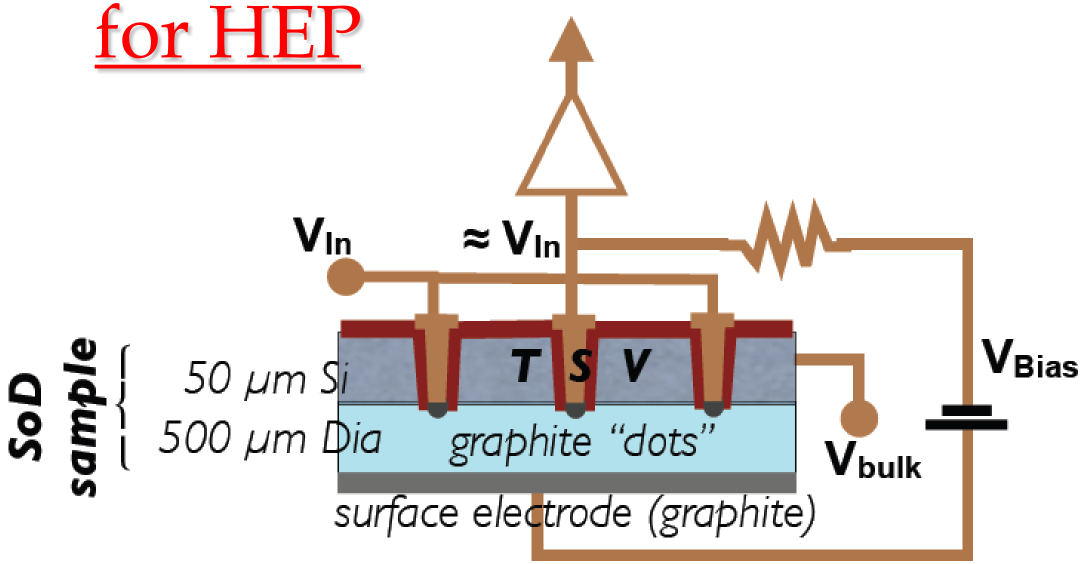

prototype-0

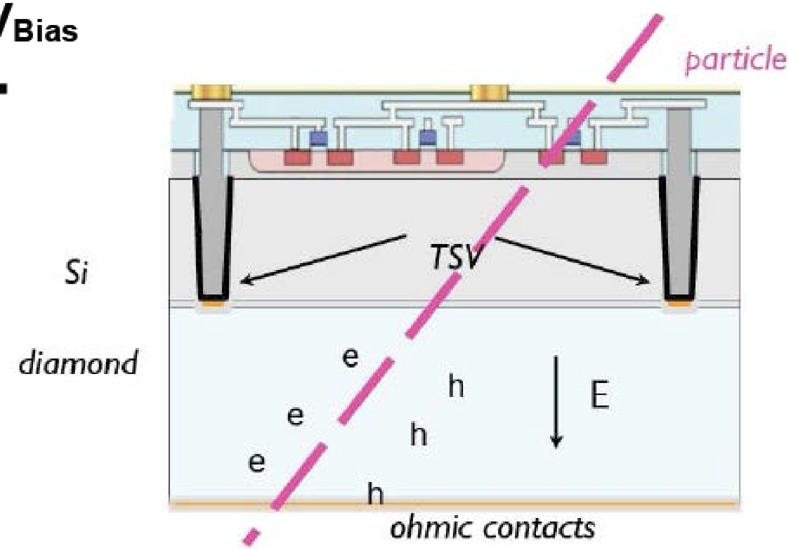

prototype-1

First SOD Prototype(s)

SOD Microelectrode Arrays (MEAs) for biological studies

Growth of neuronal cultures on diamond

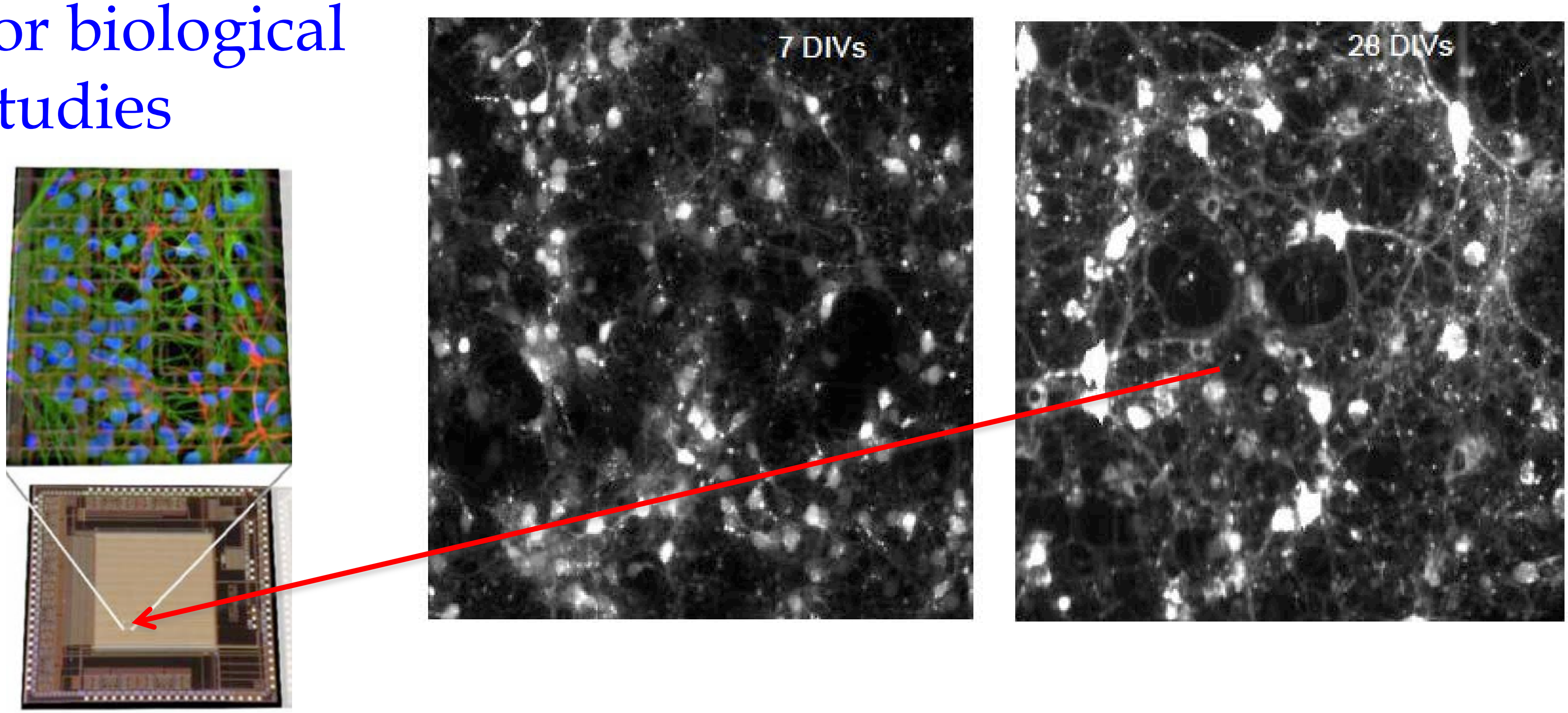

Diamond is biocompatible:
MEAs can be connected via diamond graphitic columns to neuron cultures.

First SOD Prototype(s)

Si MAPs laser-bonded on Diamond Sensors

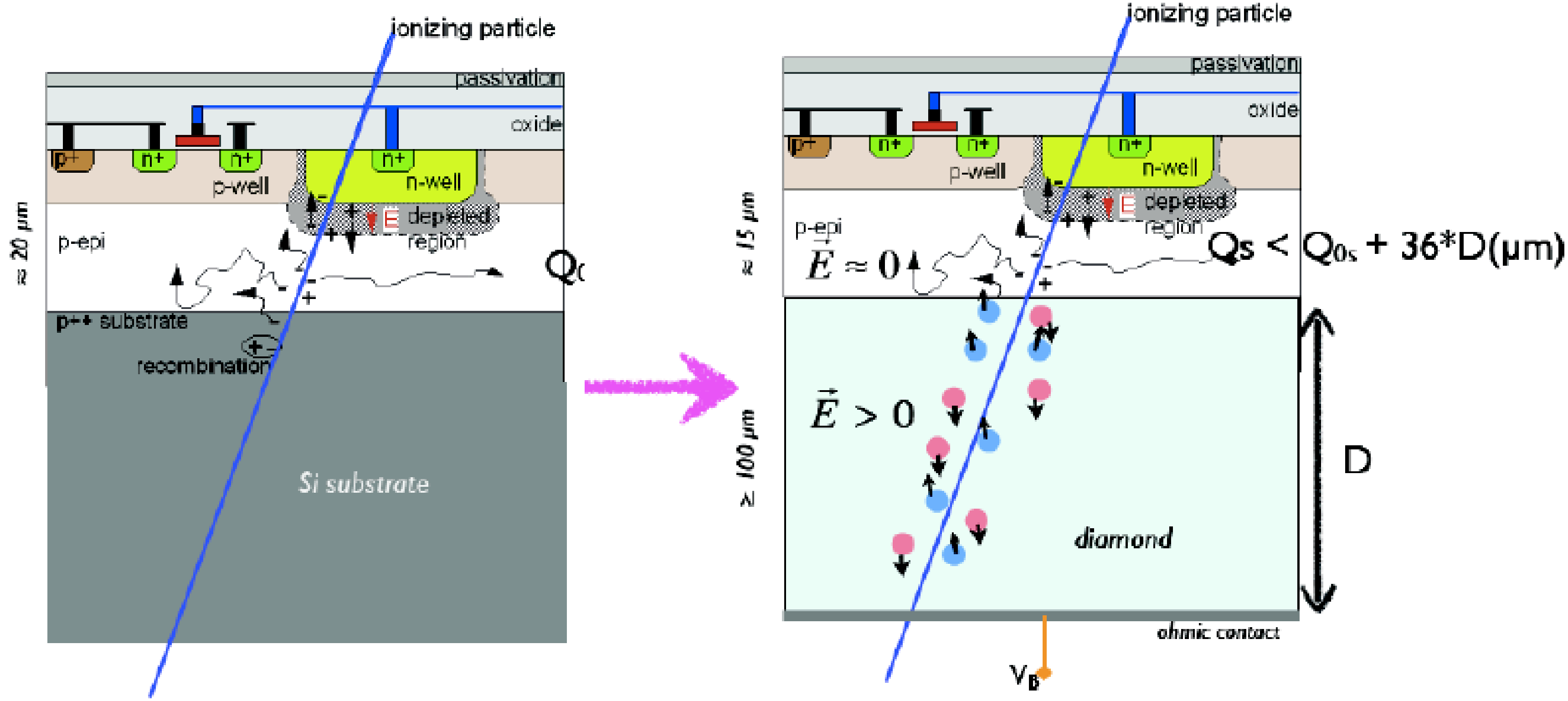

Si MAPS chip thinned to 20μm from the rear side and bonded to a (biased) diamond plate.

University and INFN Florence, S. Lagomarsino, S. Sciortino et al.

Applications in Related Fields:

Detectors for Extreme Radiation and Temperature Conditions

Neutron Sensors in Fusion Science

HSC neutron and UV-VUV detectors for JET and ITER

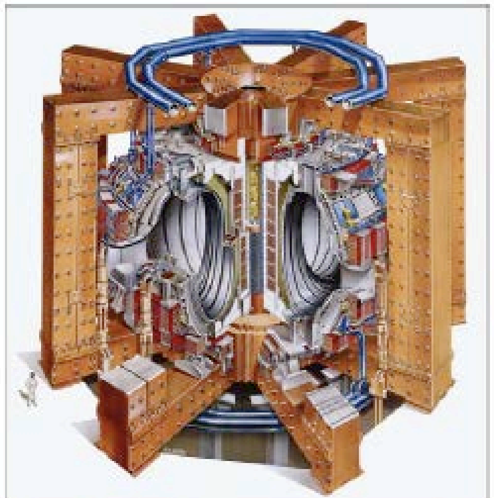

Joint European Torus (JET)
Chulam (UK)

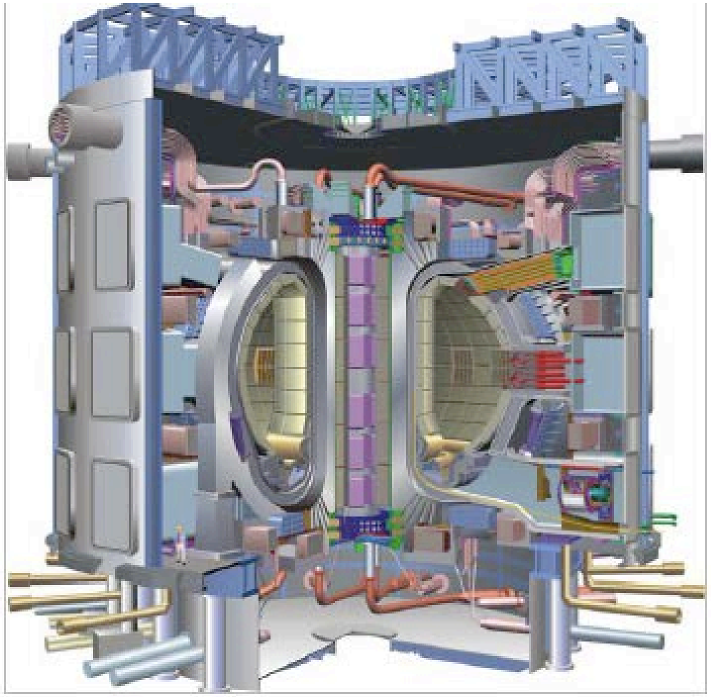

ITER

Si detectors are replaced approximately after 1 year at JET (if working with tritium).
At ITER the 14MeV neutron flux will be too high for conventional detectors:
1×10^{14} neutron/cm^2 RADIATION HARDNESS REQUIRED

D. Lattanzi et al. (2009), *Fusion Engineering and Design* **84**, pp. 1156–1159
Almaviva, S., Marinelli, M., Milani, E., et al. (2008), *J. Appl. Phys.* **103**, 054501

Neutron Sensors in Fission/Fusion

HSC for simultaneous measurements of fast and thermal neutrons

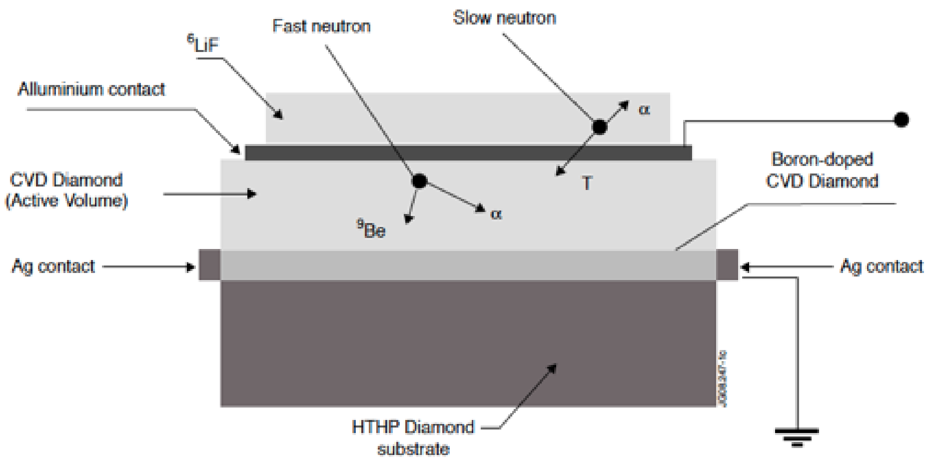

- thin B-doped layer serves for electrode
- ^{6}LiF layer on top for converting slow n.

$^{12}_{6}C(n,\alpha)\,^{9}_{4}Be$

$^{6}_{3}Li(n,\alpha)T$ $\quad$ $^{12}_{6}C(n,n')3\alpha$

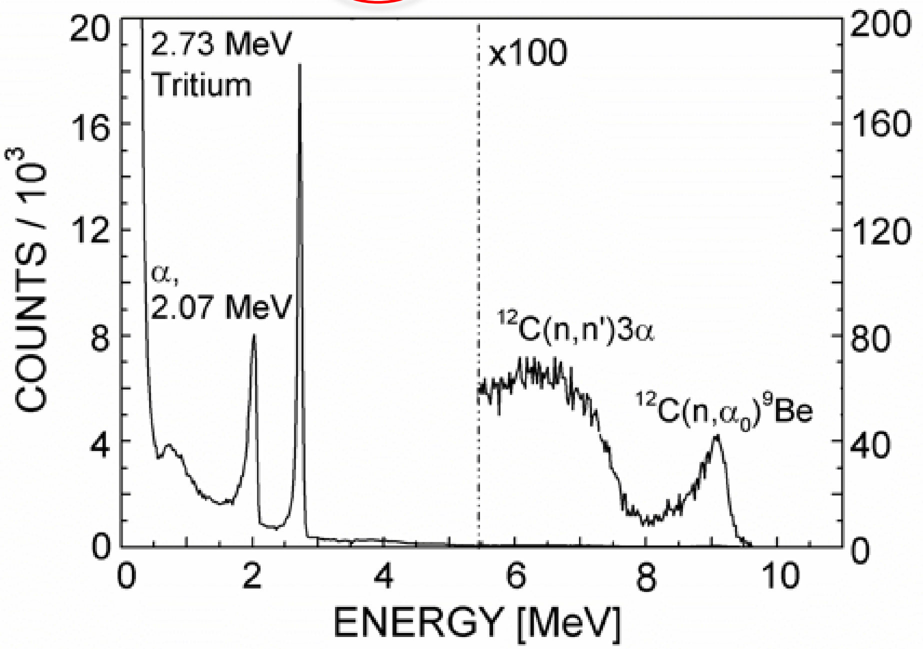

Almaviva, S., Marinelli, M., Milani, E., et al. (2008), *J. Appl. Phys.* **103**, 054501.

Position Monitors for intense, highly focused X-ray Beams (ESRF, SOLEIL, PETRA III, EXFEL)

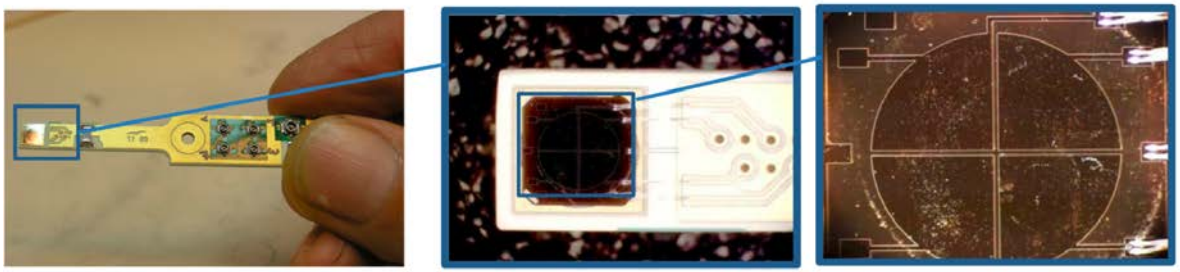

BI ≈ 10^8- 10^{10}
5-20 keV X rays
Beam spot: 0.1-50 μm

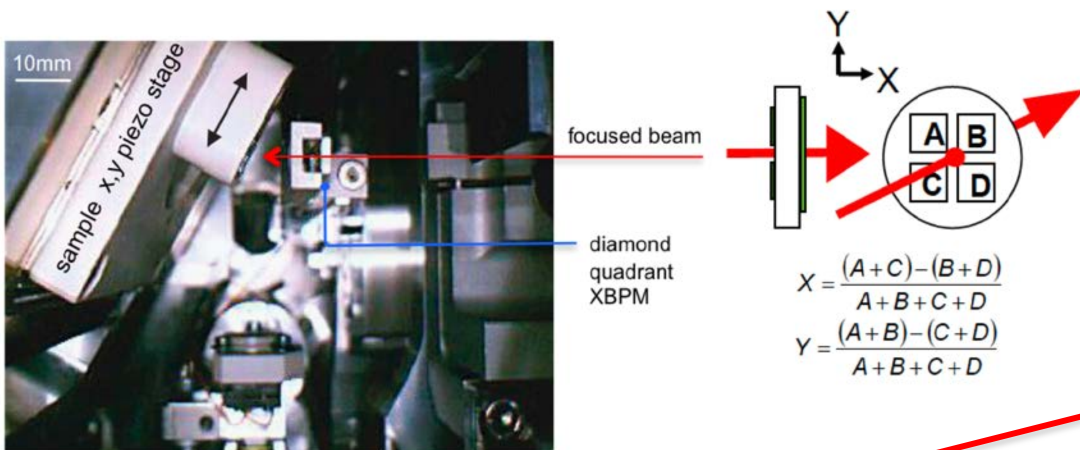

$$X = \frac{(A+C)-(B+D)}{A+B+C+D}$$

$$Y = \frac{(A+B)-(C+D)}{A+B+C+D}$$

- achieved precision:
  BP < 20 nm

XBPM at ID21 ESRF beamline

Morse, J., Solar, B., Graafsma, H. (2010), *J. Synchrotron Radiation* Vol. **17**, Iss. 4, pp. 456-464

Real-Time Monitors for the high-intensity white Beams of the NSLS

→ operating at 2.8 GeV, 300 mA

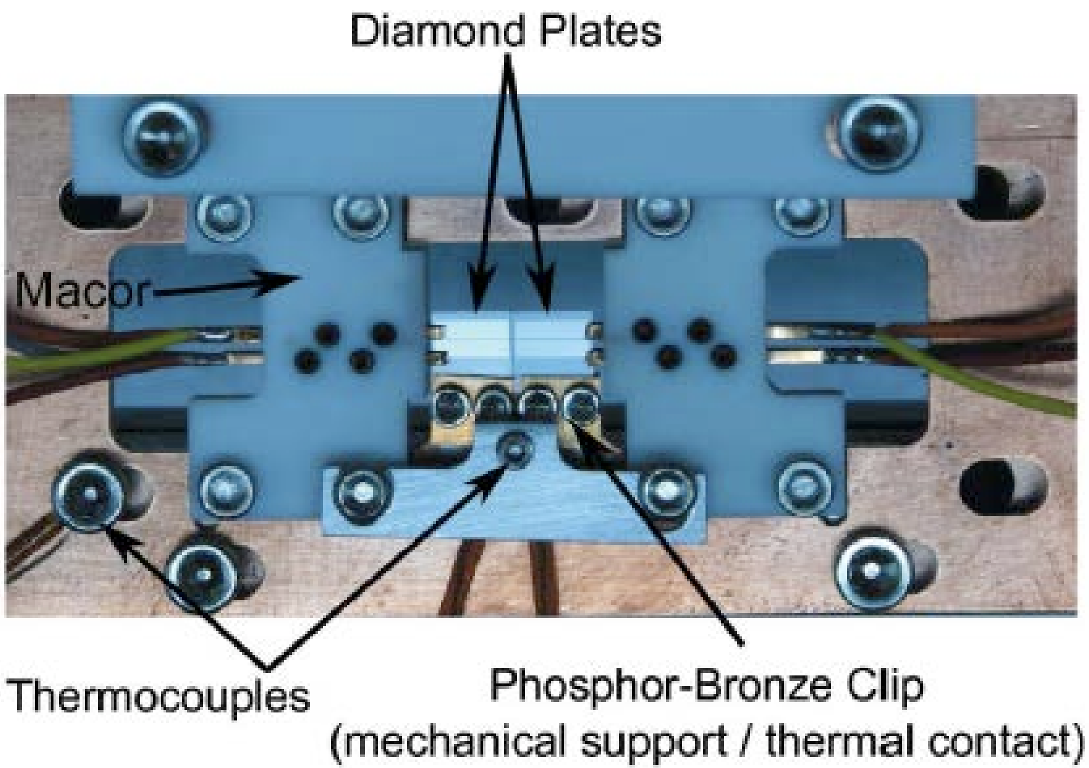

- Res.: 500nm (h); 100nm (v)

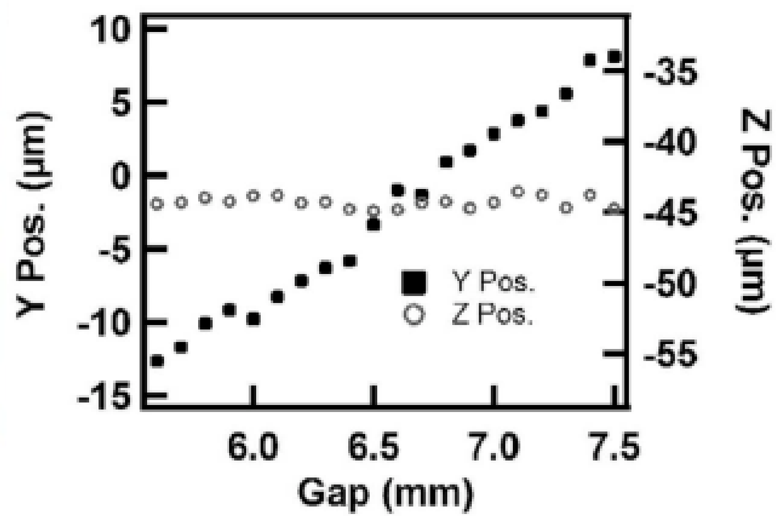

wBPM: simultaneous monitoring of flux, position, angle and timing.

Muller, E. M., Smedley, J., et al., *J. Synchrotron Radiation*, **19** (2012), pp. 381-387.

The VUV diamond sensors of the Large Yield RAdiometer (LYRA) on PROBA 2

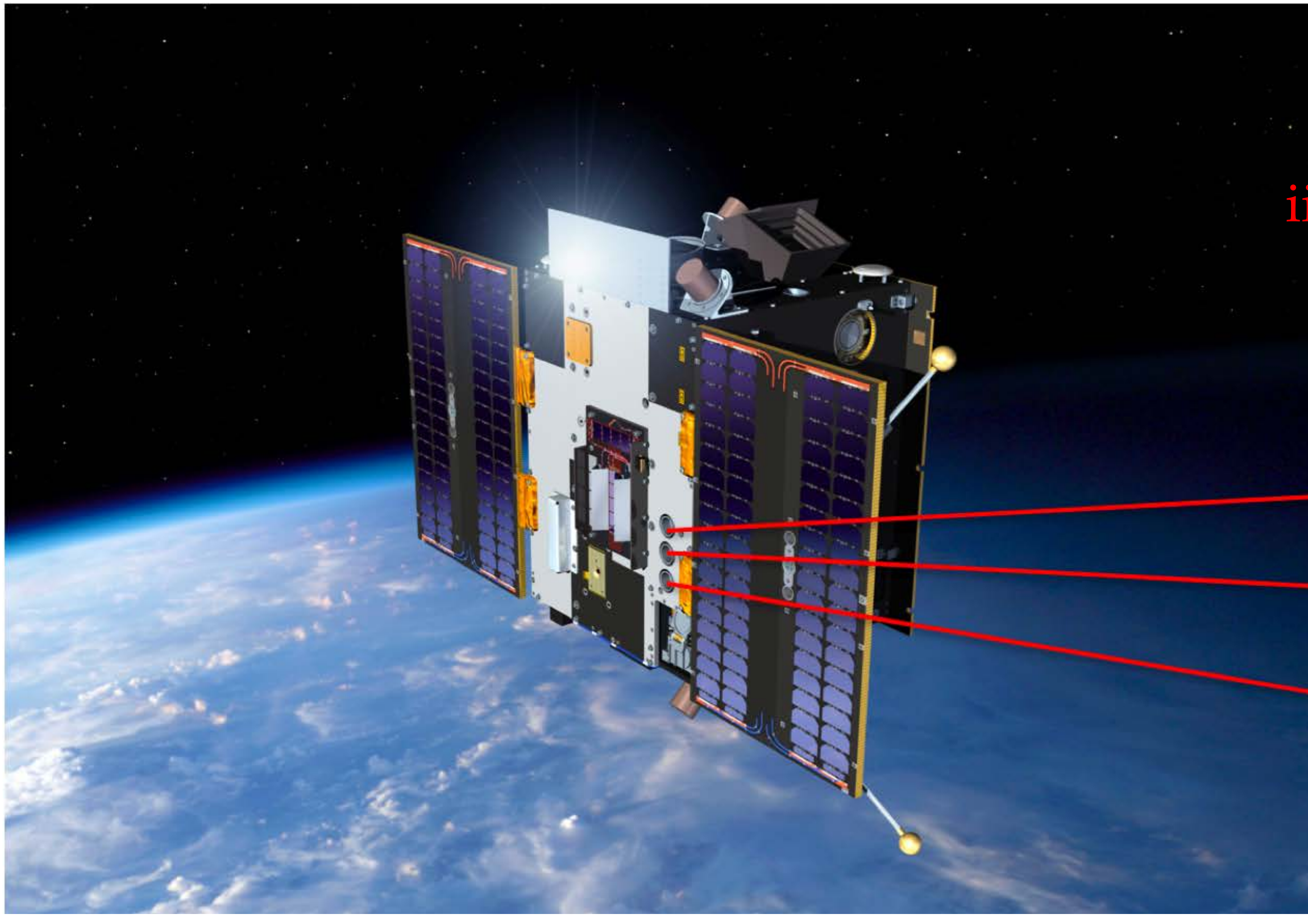

i) 1–20 nm
ii) 17–70 nm
iii) 115–125 nm (Lyman a)
iv) 200–220 nm

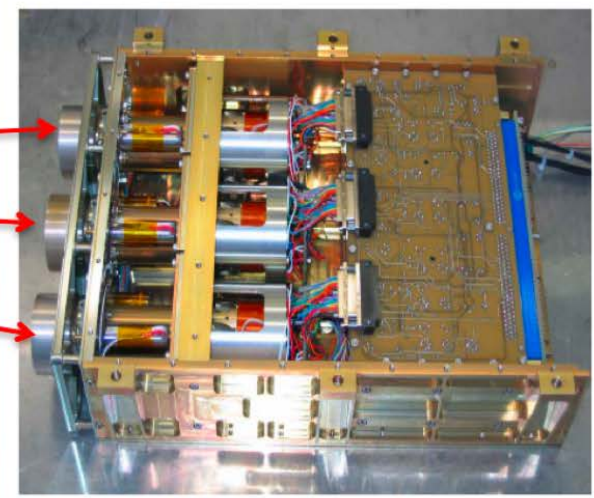

Courtesy of ESA

The VUV diamond sensors of the LYRA radiometer

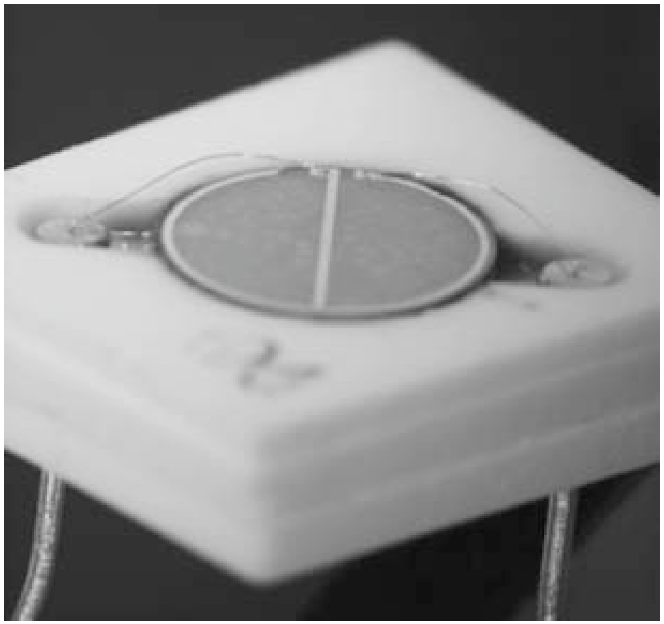

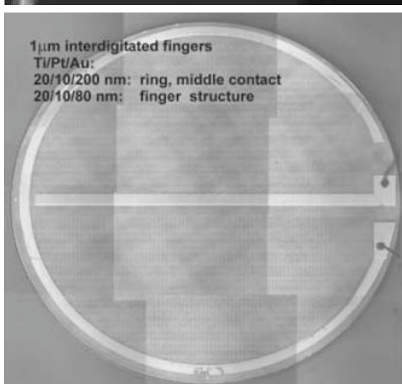

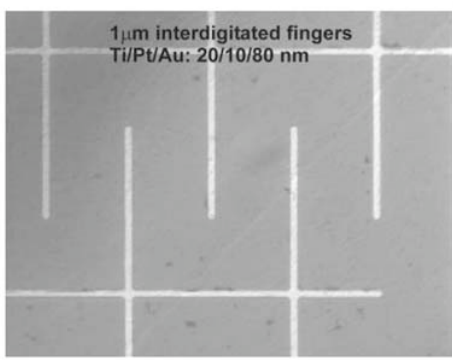

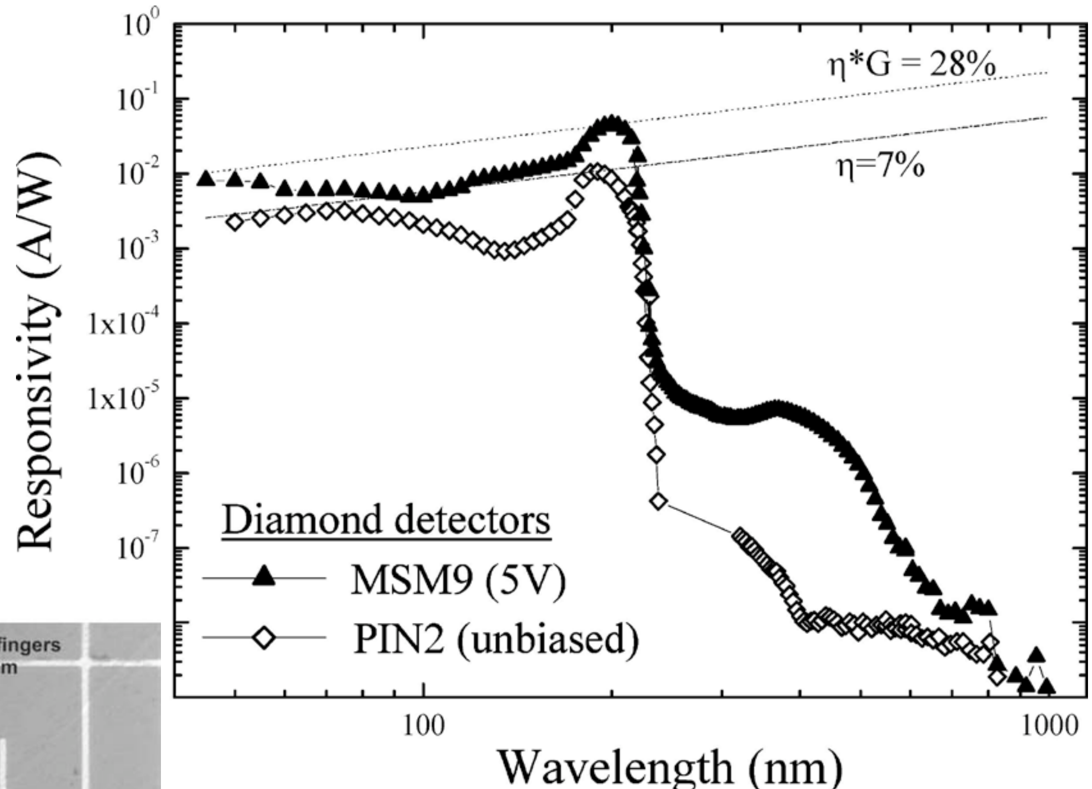

BenMoussa, A., Hochedeza J. F., et al. (2006),
Diam. Relat. Mater., Vol. **15,** Iss. 4-8, pp. 802–806

Conclusions and Outlook (LHC)

Radiation hardness studies ➡ compared:

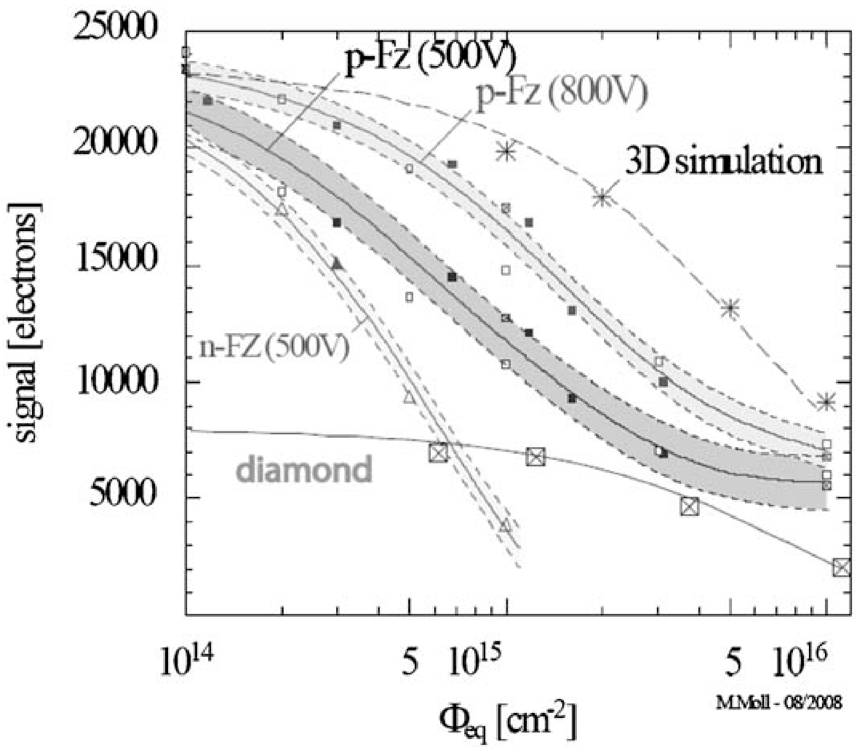

1) Silicon float zone (FZ)
with n electrodes in p bulk (p-FZ)
and p-electrodes in n bulk (n-FZ)

2) Simulations 3D devices (stars)

3) PC Diamond data
(crossed squares)

- but note: the S/N ratio may be better for diamond!

N. Wermes, 'Pixel detectors for charg
Silicon data compiled from M. Moll
3D simulations, Pennicard 2007

	25 MeV protons	24 GeV protons
$k_{diamond}$	$3.02^{+0.42}_{-0.36}$	$0.69^{+0.14}_{-0.17}$
k_{Si}	$10.89^{+1.79}_{-1.79}$	$1.60^{+0.38}_{-0.38}$

Conclusions and Outlook (FAIR)

- HI tracking and TOF: PC, wafer scale, 2D strips
- p and light ions TOF: SC, 2D strips, mod. pixels

FAR FUTURE: All applications, All designs
(except high-resolution ΔE spectroscopy)

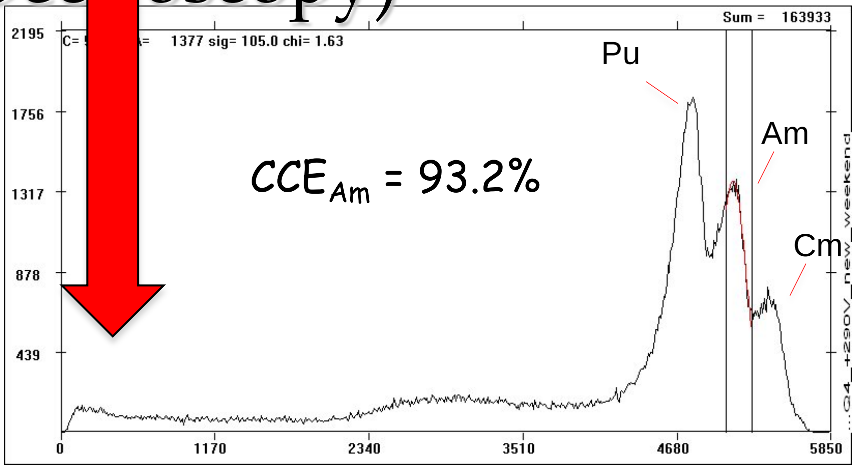

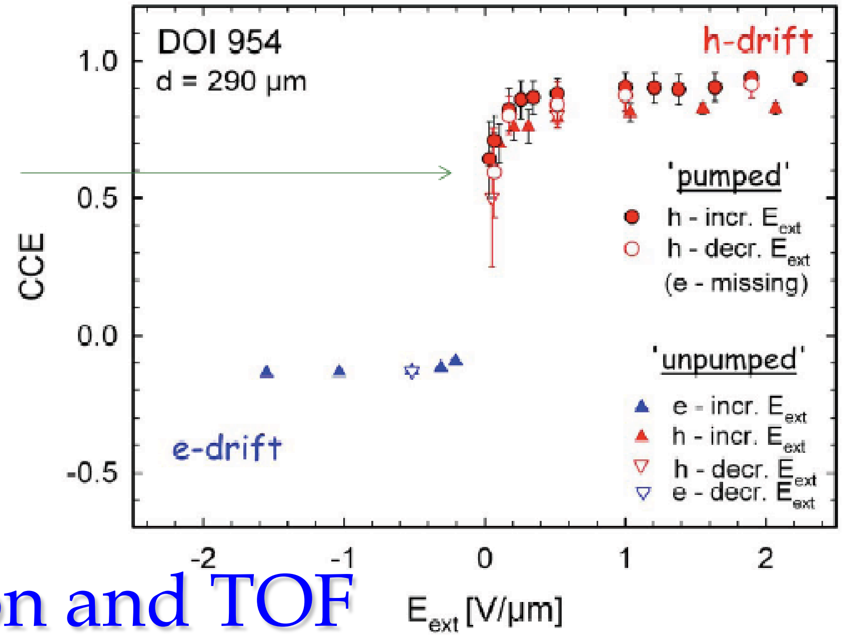

DOI: Large area,
Pulse-height resolution and TOF

The Dreams

- Large-area monolithic diamond detectors for high-resolution MIP tracking and TOF:

  Diamond sensor pixels, grown on DOI wafers with integrated FEE (i.e. with diamond electronic devices).

↓

Thin, radiation hard sensors closest connected to dedicated radiation hard FEE